Applied Physics Reviews

REVIEW ARTICLE | MAY 01 2023

MicroLED/LED electro-optical integration techniques for non-display applications

V. Kumar ; I. Kymissis

Appl. Phys. Rev. 10, 021306 (2023)
https://doi.org/10.1063/5.0125103
CHORUS

AIP Publishing

Applied Physics Reviews REVIEW scitation.org/journal/are

MicroLED/LED electro-optical integration techniques for non-display applications

Cite as: Appl. Phys. Rev. **10**, 021306 (2023); doi: 10.1063/5.0125103
Submitted: 9 September 2022 · Accepted: 20 March 2023 ·
Published Online: 1 May 2023

View Online Export Citation CrossMark

V. Kumar[a] and I. Kymissis[a]

AFFILIATIONS

Department of Electrical Engineering, Columbia University, New York, New York 10027, USA

[a]Author to whom correspondence should be addressed: vk2440@columbia.edu and ik2174@columbia.edu

ABSTRACT

MicroLEDs offer an extraordinary combination of high luminance, high energy efficiency, low cost, and long lifetime. These characteristics are highly desirable in various applications, but their usage has, to date, been primarily focused toward next-generation display technologies. Applications of microLEDs in other technologies, such as projector systems, computational imaging, communication systems, or neural stimulation, have been limited. In non-display applications which use microLEDs as light sources, modifications in key electrical and optical characteristics such as external efficiency, output beam shape, modulation bandwidth, light output power, and emission wavelengths are often needed for optimum performance. A number of advanced fabrication and processing techniques have been used to achieve these electro-optical characteristics in microLEDs. In this article, we review the non-display application areas of the microLEDs, the distinct opto-electrical characteristics required for these applications, and techniques that integrate the optical and electrical components on the microLEDs to improve system-level efficacy and performance.

TABLE OF CONTENTS

I. INTRODUCTION

The light emitting diodes (LEDs) based on InGaN/GaN semiconductors have become ubiquitous. These devices are an integral part of the solid-state lighting ecosystem including automobiles, smartphones, home lighting systems, and industrial lighting.[1–5] The adoption of LEDs has enabled additional functionalities in the form of longer lifetime, more reliable operation, smaller form factor, and lower power consumption in almost every application.

Much of the effort toward cost reduction in LEDs has been focused on increasing external efficiency using improved material growth techniques and optimizing fabrication processes.[6] The reduction in high costs of GaN semiconductor-based light emitting diodes is a challenge that needs to be addressed. Recent progress toward obtaining high-efficiency red, green, and blue LEDs using InGaN/GaN semiconductors is further paving way for new applications.[7–9]

One of the most widely anticipated applications of microLEDs and RGB capability is in next-generation self-emissive display technology.[10,11] The adoption of microLEDs in display devices is expected to enable much brighter, broader color gamut, longer lifetime, and extremely high pixels per inch (PPI) displays. A number of these characteristics are especially highly desirable in displays for augmented reality (AR) and virtual reality (VR) applications. There are multiple next-generation display demonstrations in the commercial sector. Samsung demonstrated a microLED display of 292 inches at CES 2020.[12] Jade Bird has demonstrated a microdisplay of 0.3 in. with 5000 PPI for AR/VR applications.[13] Recently, Compound Photonics unveiled a microdisplay with a record resolution of 8424 PPI.[14] The wide interest from the commercial sector to push for the next generation of display technologies using microLEDs has propelled the research effort into improving the key microLED characteristics such as efficiency, brightness, full-color emission, and lifetime.

While microLEDs have been receiving significant commercial interest for their use as emitters for display technology, little commercial focus has been applied to microLEDs for non-display applications, which is an active area of research (see Fig. 1). While high information content displays require a high resolution and small pixels, which can lead to challenges including reduced efficiency due to greater non-radiative recombination, higher current density, and degraded extraction,[15–18] many of the reviewed non-display applications can benefit from single pixel control and take advantage of relatively efficient, larger pixels. Future applications, especially in areas that benefit from ultra-small (e.g., sub micrometer) LEDs, experience some of these challenges and are briefly also discussed. MicroLEDs are increasingly being used as a signal emitter in visible light communication (VLC) systems due to their high modulation bandwidth and ability to offer parallel channels for communication using microLED array.[19–21] MicroLEDs are also well-suited for optogenetic stimulation, requiring a spatially resolved high-intensity light source.[22–24] Multiple computational microscopy techniques, such as structured illumination microscopy (SIM), for neural imaging have also used microLEDs as light sources.[25,26] The high intensity emission in the UV-blue spectrum also makes microLEDs suitable for maskless lithography.[27] These non-display applications often require modification in the electro-optical characteristics of microLEDs. Performance characteristics such as modulation bandwidth, light output power, emission wavelength, and extraction efficiency are tailored by integrating additional optical and electrical structures (see Fig. 1). The fabrication of the optical structures requires more processing on the top of the microLED structure. Despite the progress in fabrication capabilities, a number of challenges remain to be addressed for these applications.

In this review, we explore microLED electro-optical characteristics needed for non-display applications. We first discuss multiple non-display application areas highlighting key past results and ongoing research work. We then examine the performance metrics critical for the non-display applications. Definitions of the key metrics from a non-display application point of view are presented. We also highlight optical structures such as photonic crystals, microlens, quantum dots,

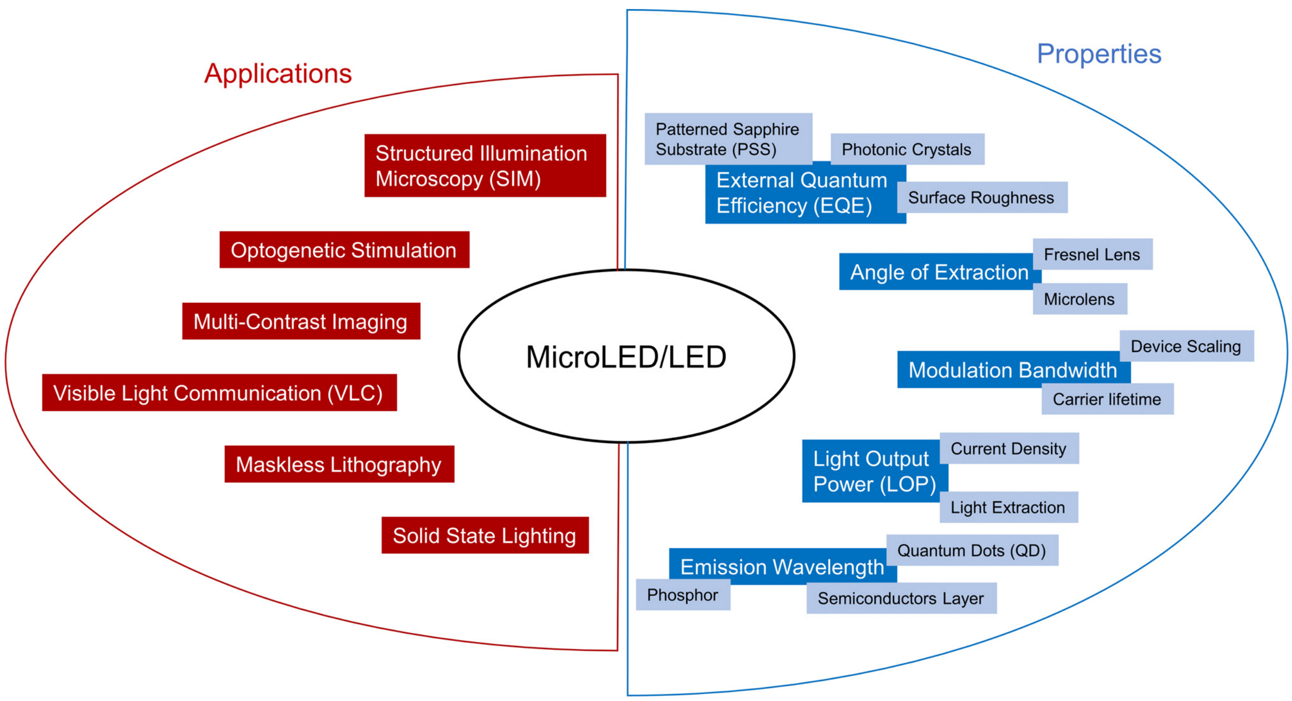

FIG. 1. A schematic diagram illustrating the correlation of key non-display applications (structured illumination microscopy, optogenetic stimulation, multi-contrast imaging, visible light communication, maskless lithography, solid-state lighting) and relevant properties of microLED/LED (external quantum efficiency, angle of extraction, modulation bandwidth, light output power, emission wavelength). It also highlights the electro-optical structures and techniques, such as patterned sapphire substrates, photonic crystals, microlenses, quantum dots, etc., required to modify the key properties.

phosphors, etc., that are needed to modify the electro-optical properties of the microLEDs. Finally, the outlook and challenges associated with the integration of advanced structures with microLEDs and their broader applications are discussed. The schematic diagram encompassing the review is shown in Fig. 1.

II. NON-DISPLAY APPLICATION AREAS

MicroLEDs have been extensively explored as pixels for next-generation displays with ultra-high brightness, deeper color gamut, and longer lifetime.[28–31] The high luminance, energy efficiency, reliability, low cost, and bio-compatibility of microLEDs also enable them to be used in various non-display technologies such as visible light communications (VLC), photolithography, optogenetics stimulation, light sources for structured illumination microscopy (SIM), and super-resolution imaging.[22,25–27,32,33] This section focuses on the system setup and recent progress of each of these applications.

A. Visible Light Communication (VLC)

The usage of microLEDs in visible light communication (VLC) systems has been investigated both as emitter devices and as photodetectors (PD).[19–21,34] The VLC system, shown in Fig. 2(c), consists of three primary components: an optical transmitter, an optical channel, and a receiver.[35] The optical transmitter contains the waveform generator, encoders, driver electronics, microLED emitters, and transmitter optics. The optical channel allows for data transfer through air or another desired medium. The receiver contains receiver optics, photodetectors, amplifiers, and decoders. The schematic diagram of a measurement setup for frequency response characterization having similar components is also shown in Fig. 2(a).

The lower RC values of microLEDs arising from their small size (1–100 μm) and short carrier lifetime result in a high modulation bandwidth. A higher 3-dB modulation bandwidth allows a higher data rate transfer in the communication system. These characteristics make microLEDs an attractive choice for optical data emitters in high-speed

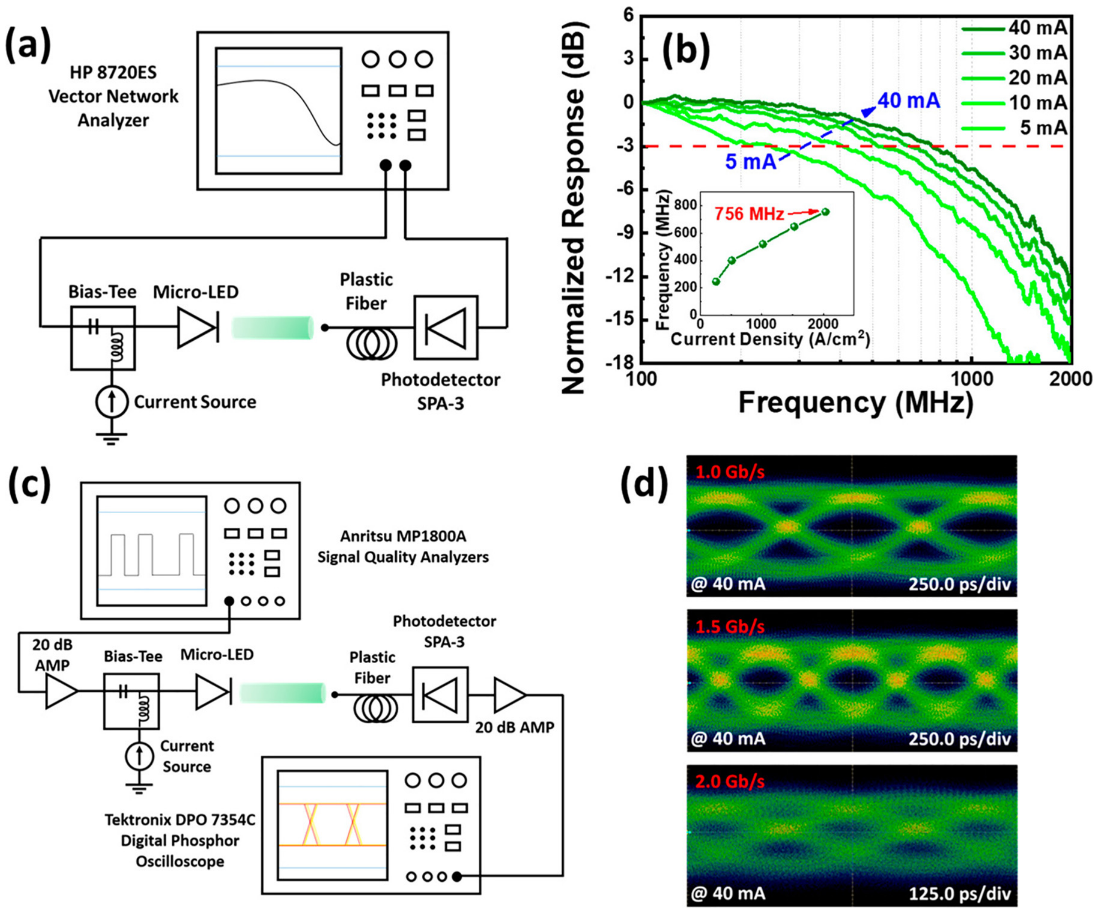

FIG. 2. The schematic diagram of a visible light communication (VLC) system. (a) The system setup to measure the frequency response of microLEDs. The system consists of a vector network analyzer, a bias-tee for operating the microLED, a plastic fiber for coupling the light, and a photodetector. (b) A plot showing improved frequency response with increasing injected current density. The current is increased from 5 to 40 mA. A maximum 3-dB modulation bandwidth of 756 MHz is shown in the inset at 2000 A/cm^2. (c) The system setup for VLC communication data-rate characterization consists of the signal quality analyzer, 20 dB amplifier, bias-tee, photodetector, and a digital oscilloscope. (d) Eye-diagram demonstrating data rates up to 1.5 Gbps with relatively higher SNR. Reprinted with permission from Chen *et al.*, ACS Photonics **7**, 2228 (2020).[35] Copyright 2020 American Chemical Society.

visible light communication systems.[36,37] The smaller mesa dimensions of microLEDs additionally facilitate higher current density operation, which was shown by McKenry *et al.* to improve high modulation bandwidth capabilities.[37] One example where an operation at higher current density (at 2 kA/cm^2) leads to a record improvement in 3-dB modulation bandwidth (756 MHz) is shown in Fig. 2(b). Additionally, 3-dB bandwidth is proportional to the increasing current density as seen in the inset of Fig. 2(b).

Data rates for VLC systems have increased from 1 Gbps to as high as 11.7 Gbps in recent works. Mckendry *et al.* demonstrated a data transfer speed of 1 Gbps in 2010 using an individually addressable 16×16 microLED array with 72 μ m diameter pixel size.[19] The blue emitter of wavelength 450 nm showed a 3-dB modulation bandwidth of 245 MHz. In 2020, Xie *et al.* demonstrated a record data transfer rate of 11.7 Gbps using a series-biased blue 3×3 microLED array.[38] This array featured smaller 20 μm diameter elements, generated over 10 mW of optical power, and displayed a high 3-dB modulation bandwidth of 980 MHz.

Many modulation schemes can be used to encode the data in the VLC systems. Most microLED VLC systems report implementing one of three key modulation schemes: Pulse Amplitude Modulation (PAM), On-Off Key (OOK), or Orthogonal Frequency Division Multiplexing (OFDM). The selection of one method depends on the prioritization of complexity or efficiency requirements. A detailed discussion of modulation schemes in VLC systems can be found in the comprehensive text by Nan Chi (2018).[39] The use of pixels with increasingly small diameters (tens of micrometers) to achieve improved data transfer rates of more than 10 Gbps in VLC systems is an encouraging sign that next-generation communication systems could be successfully implemented using microLED technology.

B. Optogenetic stimulation

Optogenetics, the technique by which light is used to selectively stimulate neural cells, has revolutionized the field of neuroscience.[40–47] It is a most widely used method to study the causal relationship between neural circuits and behavior.[46] Researchers have explored using various light transmission methods, including fiber optic cables and waveguides, to deliver stimuli to specific neuron cell populations.[48–51] These approaches can stimulate a large number of neural cells, but struggle to deliver light at a high spatial resolution, a key requirement for decoding neural circuits. Grossman *et al.* proposed a simple solution to this problem by creating an array of microLEDs capable of generating arbitrary optical excitation patterns on neuronal samples with high resolution.[52] This concept of matrix photostimulation is illustrated in Fig. 3(a). A light-sensitive ion channel known as channelrhodopsin-2 (ChR2) provides a powerful tool for millisecond neural excitation.[40] ChR2 expressing neural cells are covered with microLEDs that each has individual control over their illumination intensity and timing for optical excitation.

To gain a fuller understanding of the causal relationship between neuronal circuits and their behavior, simultaneous localized stimulation and electrical recording of neural cells are required. Such an experimental setup then must address the additional challenge of directly integrating light sources onto the stimulation sites. Scalable designs that monolithically integrate microLEDs and recording sites onto silicon neural probes can solve this problem to enable closed-loop light stimulation and electrical recordings.[53–55] Figure 3(b) shows the 48 microLED probe used by Wu *et al.* to independently stimulate distinct cells spaced 50 μ m apart.[53] Neural recordings from a freely moving mouse using this probe are also shown. Scharf *et al.* used a similar approach but increased their system's scalability by integrating

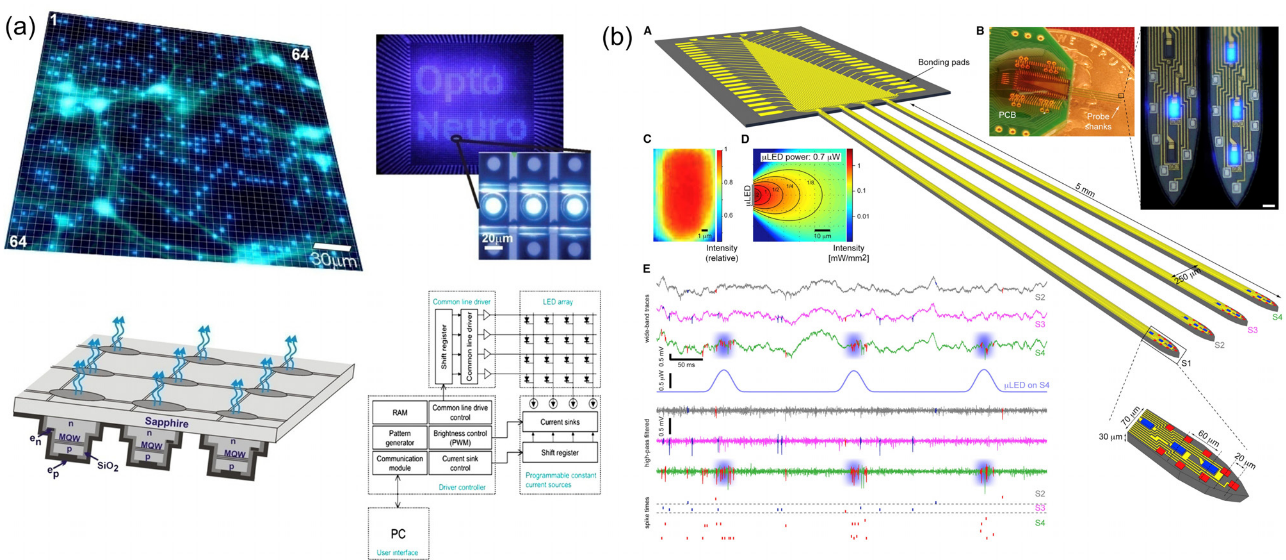

FIG. 3. (a) A 64×64 microLED array overlaid on the top of ChR2 expressing neural cells demonstrating the concept of photostimulation. Illustration of the different layers of the microLED showing p-GaN, multiple quantum wells (MQWs), n-GaN, SiO$_2$, and contacts. A schematic of the matrix addressing scheme is also shown. Reprinted with permission from Grossman *et al.*, J. Neural Eng.7, 16004(2010).Copyright 2010 IOP Publishing.[52] (b) A microLED probe driving localized spiking in freely moving mice. The probe consists of four shanks, each having three microLEDs of dimension 10×15 μm integrated with Ti/Ir recording sites to enable co-localized stimulation and electrical recording. The electrical recording from the CA1 pyramidal cell layer of a freely moving mouse is shown. Reprinted with permission from Wu *et al.*, Neuron **88**, 1136 (2015). Copyright 2015 Elsevier.[53]

96 microLEDs onto the probe.[54] The work showed depth-dependent activation with microLEDs achieving a peak irradiance of 400 mW/mm^2 at 5 mA current. McAlinden *et al.* further scaled the optrode array by creating a device with the capability to deliver light stimuli at 181 sites. This milestone was achieved by a novel fabrication method for microLEDs on GaN-on-Sapphire with glass microneedle.[56]

Tethered neural stimulation restricts the free movement of rodents. To enable untethered, remote-controlled neural stimulation and electrochemical sensing of freely moving mice, Liu *et al.* developed wireless, implantable probes with microLEDs for optogenetic stimulation and dopamine detection.[57] While these devices provide a high precision spatiotemporal stimulation method, they can cause undesirable stimulation artifacts with high enough amplitudes to mask neuronal activities.[53] Kim *et al.* demonstrated opto-electrodes capable of eliminating electromagnetic interference (EMI) induced and photovoltaic (PV) related stimulation artifacts using multi-layer metal structures and heavily boron-doped silicon substrates, respectively.[58] The application of microLEDs in optogenetic stimulation is paving the way for studies of freely moving rodents' neuronal circuits by providing compact optrodes that are essential for decoding the neural basis of behavior.

C. Structured Illumination Microscopy (SIM)

Structured illumination microscopy (SIM) allows optical sectioning imaging (OS-SIM) and/or super-resolution imaging (SR-SIM) of neural cells by modifying conventional microscopes.[59–63] It has become a widely utilized method. Its widespread use can be attributed to its relatively simple setup, which enables widefield imaging and integration with traditional microscopes. Structured illumination microscopy (SIM) uses the principle that higher spatial frequencies attenuate faster with defocus than lower spatial frequencies. For an illuminated sample with a grid projection, the modulation in the out-of-focus part of the image attenuates faster than the thin in-focus part of the image. The optically sectioned part of the image can be extracted by looking at the modulation part in the image. Figure 4(a) demonstrates how the optically sectioned part of the image can be extracted from the modulated image section. The grid moves into three equally spaced positions, sequentially capturing thirds of the image and then combining them to obtain an optically sectioned or a super-resolved image.[25]

Traditionally, this has been achieved by placing a grating grid in the illumination path and then using a piezo-based system to mechanically move the pattern and obtain phase-shifting.[64,65] The mechanical movement limits the speed and accuracy of the system. Digital micromirror device (DMD) based programmable spatial light modulators (SLMs) have been used to replace the gratings and get around the aforementioned limitations caused by slow mechanical movement.[26,66–68] These systems use lamp or LED based illumination. However, controlling illumination patterns using DMD increases the complexity of the system due to the added optical elements and increased optical path. They also suffer from the blazed grating effect that causes SIM patterns with varying intensity distribution.[69,70] The resulting SIM patterns are prone to reconstruction artifacts. Using electrically programmable microLED arrays for patterned illumination is an efficient, low-cost solution with no moving parts in a system. MicroLED based structural illumination also provides additional binning capabilities for the illumination pattern. Figure 4(b) shows a microscope setup developed by Poher *et al.* for optical sectioning using a microLED strip array as a light source.[25] The ability to use the same

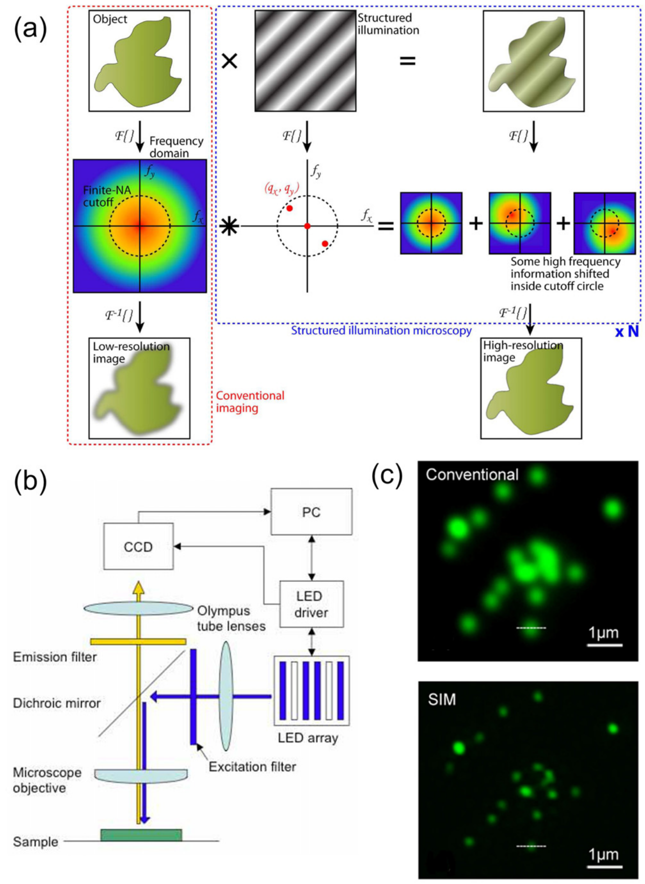

FIG. 4. (a) Concept illustration of SIM technique. In conventional microscopy, the numerical aperture (NA) limits the spatial frequency. Structured illumination shifts the high spatial frequency content of the unknown sample into low frequencies through convolution. Combining images resulting from multiple illumination patterns, a high-resolution image can be constructed. Reproduced with permission from McLeod and Ozcan, Rep. Prog. Phys. **79**, 076001 (2016).[74] Copyright 2016 IOP Publishing Ltd. (b) A microscope configuration utilized for OS-SIM using microLED stripe display as a light source. It is located in the illumination path of an Olympus microscope in critical illumination configuration to image the illumination pattern directly onto the sample. Three different illumination patterns generated by the microLED display are also illustrated 6. Reproduced with permission from Poher *et al.*, Optics Express **15**, 11196 (2007).[25] Copyright 2007 Optical Society of America. (c) Comparison of SIM with conventional microscopy. Reprinted with permission from Dan *et al.*, Sci. Rep. **3**, 1116 (2013). Copyright 2013 Springer Nature.[26]

microscope for the implementation of multiple imaging methods demonstrate a clear advantage of optical designs that use microLED array as a pattern illumination source. In addition, microLED-based light source systems could be miniaturized sufficiently to be used in miniscope designs for the neural imaging of freely moving mice which is essential for understanding the brain circuitry. A more detailed review of the SIM technique can be found in the cited articles.[71–73]

D. Other imaging techniques

Light emitting diode (LED) arrays have been used as a light source in a new type of microscope called an LED array microscope to perform computational imaging.[75–79] LED array microscope designs can be implemented by simply replacing the widefield light source of a traditional microscope with a programmable LED array. This method of computational imaging allows label-free multi-contrast, i.e., brightfield, darkfield, phase contrast, and Fourier ptychography imaging to be combined on a single platform. Brightfield contrast imaging is used to image samples with strong absorption, darkfield contrast is better suited for sub-resolution features, and phase contrast is primarily utilized for a transparent sample.[78] As different contrast modes provide different information about a sample, it is desirable to have all the imaging modes on a single hardware platform.

In traditional microscopy methods, different imaging techniques require hardware changes in the microscopy setup, while LED array microscopy provides a way to obtain different imaging modalities using a post-processing imaging algorithm without any change in the hardware. Figure 5(a) shows a time-multiplexing scheme implemented using LED arrays to obtain multi-contrast imaging. Even though these methods only require the modification of conventional microscopes to achieve different imaging techniques, optical components such as lenses and objectives make it bulky and expensive. For this reason, lens-free microscopy systems utilizing LEDs as light sources have become widely popular alternatives.[80–84] This system consists of a known and a partially coherent light source for sample illumination and an image sensor for collecting the shadow image, which is then used to reconstruct the full image. Removing the objective lens from the optical path provides a way to decouple the field of view (FOV) and resolution. In decoupled lens-free systems, the resolution is limited by the pixel size, and the FOV is determined by the active area of the image sensor. The current resolution is limited to around 1 μm.[85] This limitation can be mitigated by using techniques such as pixel super-resolution at the expense of a more complex setup.[82]

The spatial resolution of the traditional optical systems is limited due to the laws of diffraction inherent to all optical systems.[86,87] This limit is about 200 nm due to Abbe diffraction.[88,89] Various super-resolution (SR) techniques, such as photoactivated localization microscopy (PALM), stimulated emission depletion microscopy (STED), and stochastic optical reconstruction microscopy (STORM), have been explored to mitigate this fundamental limit.[74]

Another approach to pushing past this limit using LEDs is emerging as the size of the microLEDs decreases toward nanoLEDs.[90–92] The sub-micron dimensions of nanoLEDs allow them to serve as spatially resolved light sources and pave the way for Nano Illumination Microscopy (NIM).[93,94] In this technique, spatially resolved light sources are used to scan a sample by sequentially illuminating the nanoLED array and recording the optical signal through the sample on highly sensitive image sensors. Figure 5(b) shows how a sample can be imaged by measuring the intensity of light reaching an array of image sensors from each individual light source after passing through the sample. In this case, the resolution of the system is limited by the pitch of the illumination source rather than the detection system. NanoLED arrays with pitches as small as 70 nm have been demonstrated which can lead to a resolution of approximately 140 nm which is much improved than the lens-free approach with resolution limited to around 1 μ m.[85,92] With the absence of bulky lens systems, nanoLED methods could dramatically improve the form factor of super-resolution microscopy and enable a new array of applications in biological imaging.

E. Maskless photolithography

Matrix addressable microLED and LED array emitters are highly desirable as light sources for photolithography due to their ability to generate and transfer patterns on photosensitive materials without the

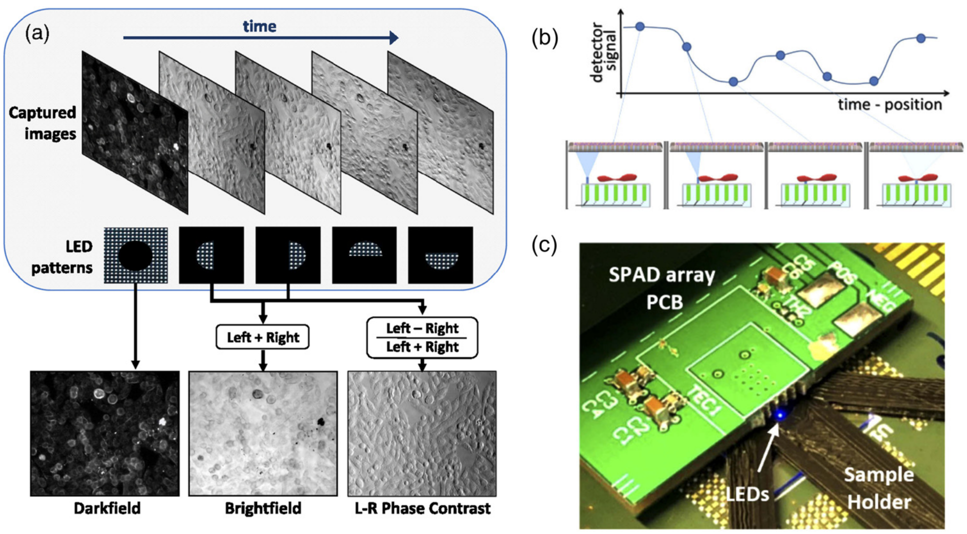

FIG. 5. (a) A time-multiplexing scheme for multi-contrast imaging in real time using LED patterns illumination. Five different illumination patterns in a sequential loop are used to obtain darkfield, brightfield, and phase contrast imaging. Reprinted with permission from Liu *et al.*, J. Biomed. Opt. **19**(10), 106002 (2014).[78] Copyright 2014 Authors, under Creative Commons Attribution 3.0 Unported License. (b) The operation principle of Nano Illumination microscopy (NIM). The sample is scanned by illuminating different nanoLEDs and a photosensor at the top detects the intensity reaching it. The resolution of this method of imaging is limited by the pixel size of the source rather than the detector which can be small beyond the diffraction limit. (c) The experimental setup for implementation of NIM. Reproduced with permission from Franch *et al.*, Opt. Express **28**, 19044 (2020).[93] Copyright 2020 Optical Society of America (OSA).

need for manufacturing expensive photomasks. As a result, it offers more flexibility in the photolithography process and a compact system. Several research groups have demonstrated the capability of microLEDs for maskless lithography.[27,33,95,96] Jeon *et al.* performed mask-free photolithography using a 64×64 UV microLED emitter array integrated with microlenses for light collimation.[33] Two circular disks with 30 and 16 μm diameters were patterned using an i-line photoresist to demonstrate the proof of concept of the integrated device. Guijt *et al.* built a simpler and cost-effective photolithographic setup with off-the-shelf UV LEDs, hardware, and optical components.[97] The system collimated light with a pinhole and plastic tube, focused on the sample with standard a microscope objective, and moved the substrate into position with a motorized linear stage. The results demonstrated direct writing lithography for rapid prototyping of features smaller than 20 μm.[97]

A similar approach utilizing off-the-shelf UV LEDs and a rotary stage was used by Suzuki *et al.* for lithography of curved microstructures.[95] This work used the inherent Lambertian distribution property of the planar LED to achieve the difference in UV exposure dose required for high-aspect-ratio and curved surface structures such as microlenses and waveguides of hundreds of micrometers of thickness.[95]

Figure 6(a) shows how Elfstrom *et al.* further advanced the technique by combining a CMOS-controlled microLED array with a projection system and translation stage to achieve written features as small as 8 μm.[27] Building further on the same setup, Guilhabert *et al.* reported mask-fee direct pattern writing with features as small as 500 nm by primarily modifying the projection optics.[96] They also showed the fabrication of InGaN micro-LEDs using the same setup. Recently, Wu *et al.* reported a UV micro-LED display with full high-definition of 960×540 and 1920×1080 for pattern-programmable maskless photolithography on resist-coated wafers.[98] Figure 6(b) shows the microLED display and a patterned Si substrate using maskless lithography. All these reports show the potential of microLED technology for photolithography applications that require minimal setup and provide a budget-friendly alternative to traditional laser-based systems.

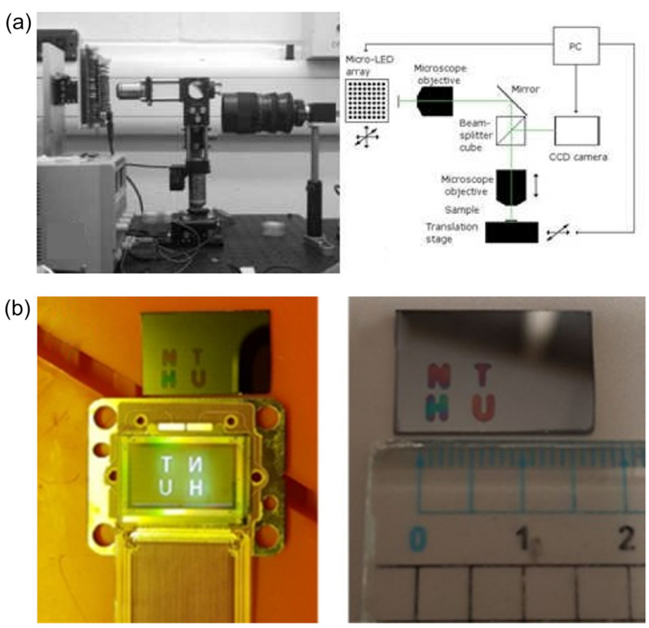

FIG. 6. (a) A micro-projection system used for maskless UV photolithography. The system consists of CMOS driven microLED array, a horizontally mounted objective for light collection, a 45° mirror for directing light downward, a vertical objective, and a piezo-driven stage for z-translation for focusing. Reproduced with permission from Elfström *et al.*, Opt. Express **17**(26), 23522–23529 (2009).[27] Copyright 2009 Optical Society of America. (b) Mirror pattern of letter "NTHU" programmed on a 1920×1080 microLED display and then revealed on a photoresist coated Si wafer using maskless photolithography. Reproduced with permission from M.-C. Wu and I.-T. Chen, Adv. Photonics Res. **2**, 2100064 (2021).[98] Copyright 2021 Authors, licensed under a Creative Commons Attribution 4.0 License.

TABLE I. Non-display applications reviewed and enabling primary performance characteristics.

Application	Properties
VLC	Efficiency, modulation BW
Optogenetics	Size/implantability, Output power
SIM	Output power, beam shaping
Imaging	Output power, pattern control
Maskless photolithography	Intensity, wavelength control

III. PERFORMANCE METRICS FOR NON-DISPLAY APPLICATIONS

The various applications discussed in Sec. II have different primary enabling performance properties. Table I summarizes the reviewed non-display applications and the key desirable properties. MicroLED technology offers superior performance than organic light emitting diodes (OLEDs) for key properties such as brightness, response time, and lifetime. Table II summarizes the performance comparison between the microLEDs and OLED technology.[99] Many of the metrics, such as superior brightness, reliability, and lifetime, make microLEDs well-suited to both display and non-display, but some of the key performance metrics for non-display applications differ from those for display applications. This section discusses the key performance parameters of microLEDs that must be optimized or enhanced for non-display applications. These metrics include optical extraction, angle of extraction, modulation bandwidth, light output power, and response time.

TABLE II. Performance comparison of key properties between OLED and microLED technology.[99]

Properties	OLED	MicroLED
Mechanism	Self-emissive	Self-emissive
Brightness	1000 Cd/m^2	10^6 Cd/m^2
Lifetime	30 000 h	100 000 h
Response time	Microsecond	Nanosecond
Pixel density (PPI)	up to 2500	up to 30 000
Energy	Medium	Low
Cost	Low	High

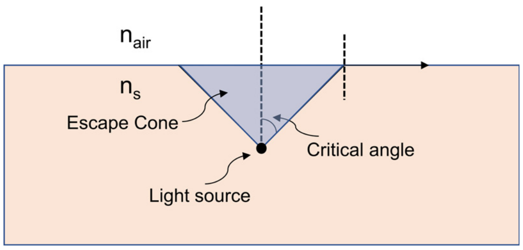

FIG. 7. A schematic diagram showing the concept of escape cone. The escape cone at the semiconductor with refractive index n_s and the air with refractive index n_{air} interface is defined by the critical angle. Only the light inside the escape cone is eventually emitted from the active region of the microLED; everything else is reflected back into the semiconductor and reabsorbed, leading to a low extraction efficiency.

A. Optical extraction efficiency—EQE vs IQE

Blue microLEDs have internal quantum efficiencies (IQEs) that can exceed ninety percent as a result of advances in growth techniques that have yielded high-quality materials and crystal structures.[100–103] However, the external quantum efficiency (EQE) of GaN-based microLEDs, defined as the ratio of the number of photons emitted vs the number of photons internally generated, is comparatively low with a peak EQE of generally smaller than 15%.[104–106] The EQE of the microLEDs can be viewed as the product of two separate efficiencies: IQE and light extraction efficiency (LEE).[107] While IQE is significantly improved over the years, LEE has been a limiting factor.[100,108,109] Low LEE is primarily due to the large refractive index difference between air and semiconductors that traps light from total internal reflection (TIR) and Fresnel loss at the interface.[110] For example, the external efficiency could be as low as 4.3% in a typical semiconductor material with a refractive index of 2.4. Figure 7 graphically demonstrates how only the light inside the escape cone, defined by the critical angle, is able to escape. This limitation presents a challenge for microLEDs in applications such as optogenetic stimulation because the photosensitive opsins often require minimum irradiance (typically in the range of 10–100 mW/cm^2 in instantaneous light intensity) to be delivered at the neurons for activation and fluorescence.[111,112] Achieving the desired optical power numbers with smaller microLEDs requires improvements in the external efficiency of the microLED. A number of techniques to overcome the limitation of low EQE are discussed in Sec. IV A.

B. Angle of extraction

One critical metric for non-display applications is the angle of the light emitted from the active region of the microLED source. Planar microLEDs exhibit a Lambertian output distribution at the source by default, which is advantageous for wide-viewing applications such as displays.[113,114] On the other hand, applications like structured illumination microscopy (SIM) require that the light extraction cone be as narrow as possible. A lower numerical aperture (NA) is needed to prevent any light leakage into an adjacent pixel or row.[62,63] A narrower light beam is also needed to better couple the light into the optical systems and control the optical path.[115] A wider extraction cone decreases coupled light into the optical system and, thus, the overall optical efficiency of the system. Removing collimating optics, as seen in the system in Fig. 8(a), is advantageous in decreasing the complexity and bulkiness of the system overall.[116] Additionally, Sun *et al.* also showed that the presence of photonic crystals can narrow the light

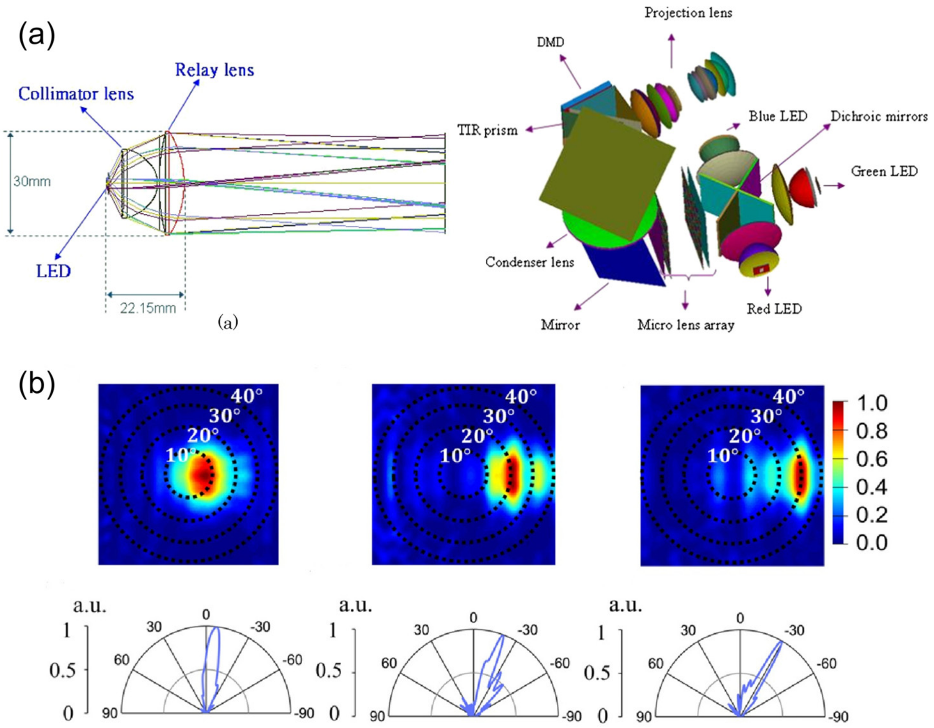

FIG. 8. (a) The need for a collimator and relay lens to collect and collimate all the light from wide angle cone source. Reprinted with permission from Sun *et al.*, Appl. Opt. **53**, H227 (2014). Copyright 2014 Optica Publishing Group.[116] (b) Narrow beam of light with far-field emission cone of 10°, 20°, and 30°, using *in situ* resonant cavity and metasurfaces. Reprinted with permission from Huang *et al.*, Opt. Lett. **46**, 3476 (2021). Copyright 2021 Optica Publishing Group.[118]

distribution and remove the need for an additional lens system to collect and collimate light.[116] In another work, Iyer *et al.* showed unidirectional luminescence from InGaN/GaN quantum well metasurfaces at arbitrary engineered angles.[117] Huang *et al.* further developed this idea by proposing a single-chip microLED with unidirectional emission that integrates the resonant cavity and metasurfaces for potential application to 3D displays.[118] The usage of the resonant cavity and metasurfaces *in situ* provides an additional tuning parameter to generate unidirectional emission with controllable full width at half maximum (FWHM), achieving angles as narrow as 10°, 20°, and 30° as shown in Fig. 8(b).

C. Modulation bandwidth

The bandwidth of a communication system is a key determining factor of its maximum achievable data transfer rate. In this context, the 3-dB modulation bandwidth of microLEDs is the most important factor for visible light communication systems as an optical signal emitter. The modulation bandwidth is determined by the carrier lifetime of the emitter and the RC time constant, where R is the differential resistance and C is the device capacitance.[36,37] The lower RC values of microLEDs arising from their small size and short carrier lifetime result in a high modulation bandwidth that can easily reach several hundred MHz.[37,119,120] A plot of modulation bandwidth against current density for various mesa dimensions is shown in Fig. 9. The modulation bandwidth initially increases with the current density because carrier lifetime is the dominant factor determining the bandwidth. At a higher current density, the RC time constant becomes a dominant factor limiting the current density.[121,122] At the desired current density, either one of the dominant factors can be improved to increase the modulation bandwidth for the VLC system.

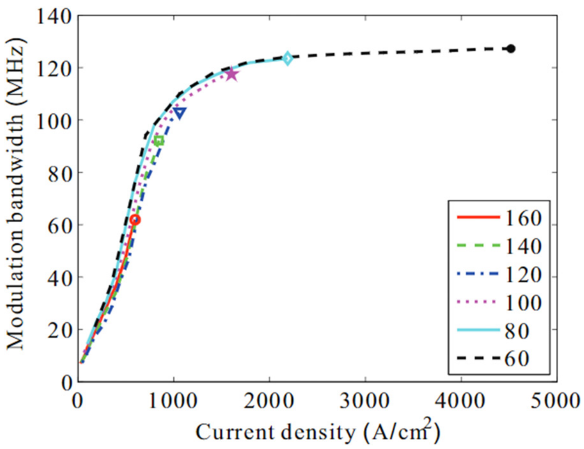

FIG. 9. A graph showing the 3-dB modulation bandwidth of microLEDs as a function of current density for different pixel sizes ranging from 60 to 160 μm. The modulation bandwidth initially increases as the current density of microLED increases and then saturates for higher current density operation. The smaller pixel sizes achieve higher modulation bandwidth as they can be operated at higher current density. The markers on the plot denote the maximal modulation bandwidth in the measurement for each size. Reproduced with permission from Huang *et al.*, Phys. Status Solidi A **215**, 1800484 (2018).[122] Copyright 2018 WILEY-VCH Verlag GmbH & Co. KGaA, Weinheim.

D. Emission wavelength

Tuning microLED light emission to a particular wavelength is highly desirable for many non-display applications.[20,55,58,98,123] Apart from the need for red, green, and blue emissions for full-color microLEDs displays, it is also required for solid-state lighting and white light communication systems.[124,125] There are three primary ways to modify light emission wavelength: through phosphors, using quantum dots (QDs), or by changing the compound semiconductor layer itself.[126–129] These techniques are discussed in detail in Sec. IV C. The wavelength of the light emitted from the microLEDs is also an important factor for optogenetic stimulations. The light-sensitive proteins, i.e., opsins, are sensitive only to a certain range of wavelengths. It is important to match light emission to the maximally sensitive wavelength of these proteins.[130] For example, channelrhodopsins (ChRs) absorption peaks range from 440 to 590 nm, and other retinal-binding proteins show peaks from 630 to 644 nm.[131–136] Emission wavelength is similarly important for photolithographic applications because photoresist must be exposed at wavelengths in the UV region for proper development.[137,138]

E. Light Output Power (LOP)

The light output power of microLEDs is one the most important factors for applications including solid-state lighting, optogenetics, imaging, and photolithography.[21,97,139,140] The light-output power of microLEDs initially increases as we increase injected current density but then saturates and further decreases as the current density is increased.[139,141] This is due to the self-heating effect that causes increased non-radiative recombination and carrier leakage.[141,142] As mentioned earlier, in optogenetics applications, there is a minimum light output power required at the neurons for the photosensitive proteins to stimulate action potentials.[111,112] Even though microLEDs can operate at much higher current densities (>1 kA/cm^2) than LEDs, the total light output power (LOP) is smaller due to their small size.[143] If an optogenetic application requires deeper tissue stimulation, the optical output power of microLEDs becomes even more important.[134] Thicker photoresists used in photolithography also require higher light output power for adequate exposure.[137]

IV. OPTICAL STRUCTURES FOR IMPROVED PERFORMANCE

Despite the superior performance of microLEDs when compared with OLEDs, modification in the key properties of microLEDs is often required for non-display applications. Electro-optical components such as photonic crystals, nanostructures, microlenses, Fresnel lenses, quantum dots, phosphors, etc., are integrated with the traditional microLEDs to improve the output performance. Key optical components that can enhance the performance metrics of microLEDs and make them more suitable for use in non-display applications are discussed in Secs. IV A–V.

A. Extraction efficiency enhancement

The low extraction efficiency of microLEDs originates from the traditionally grown epilayer structure of the GaN LEDs.[6,106,144] A typical GaN epi structure is grown hetero-epitaxially on a sapphire substrate due to the lack of availability of a suitable substrate for homoepitaxial growth.[145,146] The photons generated inside the GaN layer with high refractive index ($n \approx 2.4$) undergo total internal reflection (TIR) at the GaN-air interface. This consequently reduces the overall efficiency of the extracted light.[147] Researchers have suggested methods including chip shaping, photonic crystals, surface roughness, and mesa shape modification to improve the extraction efficiency of microLEDs.[148–152] This section discusses the techniques for extraction efficiency enhancement in the context of various non-display applications.

1. Photonic crystals

Photonic crystals (PhCs) are repeated dielectric structures of length scales similar to the wavelength of light.[148,153,154] These crystals have the capability to modify spontaneous light emission by creating a photonic bandgap that can interact with the electronic bandgap of the emission material.[155] The photonic bandgap can be utilized in two ways to increase the extraction efficiency: inhibiting the emission of the guided modes or redirecting trapped light into radiated modes. The photonic crystals should be physically very close to the active light emitting region to maximize their impact. Wierer *et al.* demonstrated electrically operated InGaN/GaN LEDs with photonic crystals having a tunnel junction to provide lateral current spreading to the photonics crystals.[154] This work reports increased microLED radiance and an approximately 1.5x total increase in light extraction with photonic crystals incorporation. Additionally, the far-field radiation pattern of LEDs with PhC was also radically different than planar LEDs.[154]

Oder *et al.* demonstrated extraction efficiency enhancement of 63% in InGaN/GaN blue (460 nm) microLEDs and 95% in AlInGaN/GaN UV (340 nm) microLEDs. These results were achieved by patterning triangular arrays of photonic crystals with electron beam lithography.[156] Meanwhile, Kim *et al.* reported GaN LEDs with square-lattice 2D photonics crystals patterned using laser holography (LH) method suitable for high-throughput and large area processing.[157] Figure 10(a) shows the photonic crystals and the schematic diagram of the fabricated device. Enhancement in the light output of up to 2.6× is observed in the device integrated with photonic crystals of lattice constant 500 nm, as seen in Fig. 10(b). In other works, researchers have fabricated photonic crystals on pGaN using monomer-based nanoimprint lithography. These LEDs showed a 2.6× times increase in photoluminescent intensity compared to LEDs without the photonic crystal patterns.[158]

McGroddy *et al.* reported increased directional emission by 3.5× using optimized 2D photonic crystals.[159] These devices have additional index guiding layers in the vertical direction that take advantage of directionality and guided mode control.[159] Photonics crystal-based LEDs rivaling the best of the non-photonic-crystal LEDs have also been shown along with the theoretical electromagnetic calculations matching the measured results.[148] Photonic crystals fabricated on the top of the surface of LEDs suffers from limited interaction with lower order modes resulting in a poor extraction of a relatively high portion of light carried by low order modes.[160,161] Matioli *et al.* proposed embedded air-gap PhCs within the LEDs for much greater interaction with low order modes to improve extraction efficiency further.[153] Improvements as much as 8.3× has been shown using complex photonic structures through simulations in the recent past.[149]

2. Surface roughness

Textured, rough surfaces increase the extraction efficiency of microLEDs by increasing the angular randomness of the photons inside the light emitting diode. This randomization provides multiple opportunities for the photons to enter the escape cone.[162] Various research groups have reported on increasing light extraction efficiency using surface roughness.[162–171] Schnitzer *et al.* demonstrated an EQE of 30% using a textured surface and a rear metallic reflector to enhance angular randomization.[162] Windisch *et al.* experimentally investigated the transmission properties of a textured surface to achieve 2× increase in angle-average transmission and used it to achieve 46% external extraction efficiency in unencapsulated light emitting diodes.[163] Other methods created textured surfaces with natural

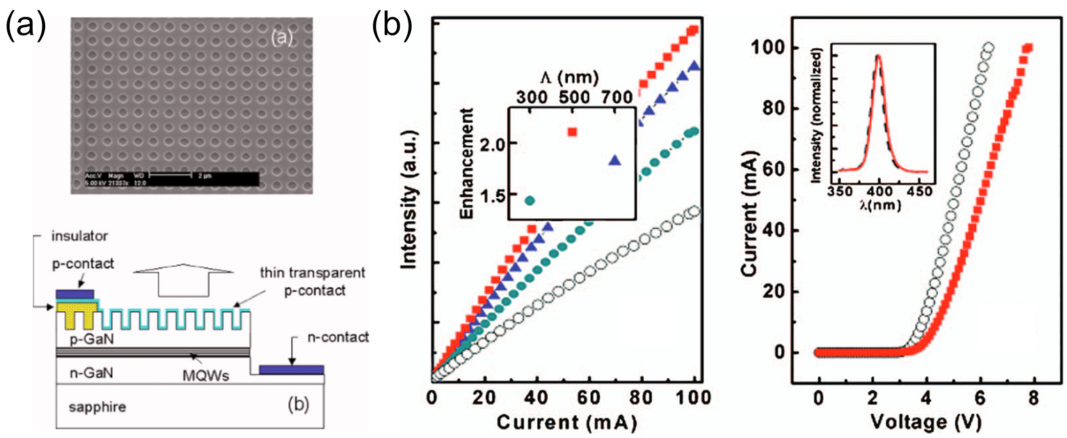

FIG. 10. Photonic crystal integration with microLEDs. (a) SEM image of air-hole photonic crystals patterned using holographic double exposure on the top of an LED structure. The PhC has a lattice period of 700 nm. The schematic diagram of the PC-LED is also illustrated in the FIG. The photonic crystals are patterned in the pGaN material with a thin transparent p-contact layer on the top as a current spreading layer. (b) Light output intensity vs injected current density plot for photonic crystals with lattice periods 300, 500, and 700 nm and a reference LED with no PhC. An enhancement of up to 2.6× is observed in the light output. A second graph shows the current-voltage characteristics of the reference microLED and the PC-LED with a lattice period of 500 nm. Reprinted with permission from Kim *et al.*, Appl. Phys. Lett. **87**, 203508 (2005).[157] Copyright 2005 American Institute of Physics.

lithography techniques that used polystyrene spheres as a dry etch mask.[171,172] Improved light output and electrical performance were also observed after microroughening the pGaN surface using metal clusters as etch masks during wet etching.[164]

A typical GaN LED structure consists of a thin pGaN layer on the top and a nGaN layer grown on a sapphire substrate. While it is easier to roughen the pGaN surface at the top, Fuji *et al.* were able to use flip-chip bonding and laser liftoff (LLO) to access the nGaN surface for roughening. They demonstrated a 2.3× improvement in the total output power compared to that of a non-roughened LED.[165] Figure 11 shows the roughened nGaN surface and the resulting improvement in the performance of an LED with the increase in surface roughness.[165] Double-sided roughening of both the pGaN layer and the undoped layer can increase the randomization of the photons and further improve light output.[166] Chang *et al.* went beyond the typical etching process and used femtosecond laser ablation to create nanostructures on the surface to increase light output from LEDs by 18%.[169] A recent computational study comparing the effectiveness of surface roughening with that of integrating photonic crystals shows that photonic crystals can create higher light extraction improvements, but the ease of fabrication to create surface roughness still makes it a compelling method to improve light extraction from light emitting diodes.[170]

3. Patterned Sapphire Substrate (PSS)

Light emitting diodes grown on commonly used c-plane sapphire substrates suffer from high defect density in epilayers due to a large mismatch between the lattice constant and thermal expansion coefficients of sapphire and GaN.[144] These differences are responsible for degrading external quantum efficiency.[144] Patterned sapphire substrates (PSS) featuring different types of artificial structures have achieved notable progress toward solving these problems.[140,173–175] The microscale structures are generally created using conventional dry etching or wet etching methods; and nanoscale structures are fabricated using nanospheres, nanoimprint lithography, or anodic aluminum oxide techniques.[176–180] PSS have several advantages over flat sapphire substrates. PSS provides a versatile platform for the growth of visible and UV epilayer structures, requires no interruption during the growth process, reduces the density of threading dislocation in epilayers, and enhances light extraction efficiency due to the increased probability of light scattering.[181] PSS has also been shown to suppress the quantum confined stark effect (QCSE) and improve UV-LED external efficiency.[182–184] Figure 12 shows a UV-LED with PSS incorporated.[182] As seen in the comparison plot, UV-LED with PSS has a higher output power than a conventional LED at the same injected current. The origin of the improved light output power is attributed to the reduction in threading dislocation (TD) induced non-radiative recombination as well as enhanced light extraction due to scattering. Increased light output power with pyramidal patterns at both micro- and nanoscale has been reported.[185] Nanoscale patterns show more improvement in output power than microscale patterns. PSS growth techniques, shape, pattern size, spacing, aspect ratio, and other parameters have considerable influence on epilayer quality and eventual LED performance. A detailed review of the subject has been presented in the literature.[181]

B. Beam shaping

Planar microLEDs have a Lambertian light output distribution.[113,114] The luminous intensity of a Lambertian surface is proportional to the cosine of the angle between the observed direction and the surface normal. The radiant intensity of such a surface is the same when viewed from any angle. Uniform radiant intensity is advantageous for wide viewing applications such as displays or TVs. Other non-display applications such as SIM, optogenetic stimulation, or

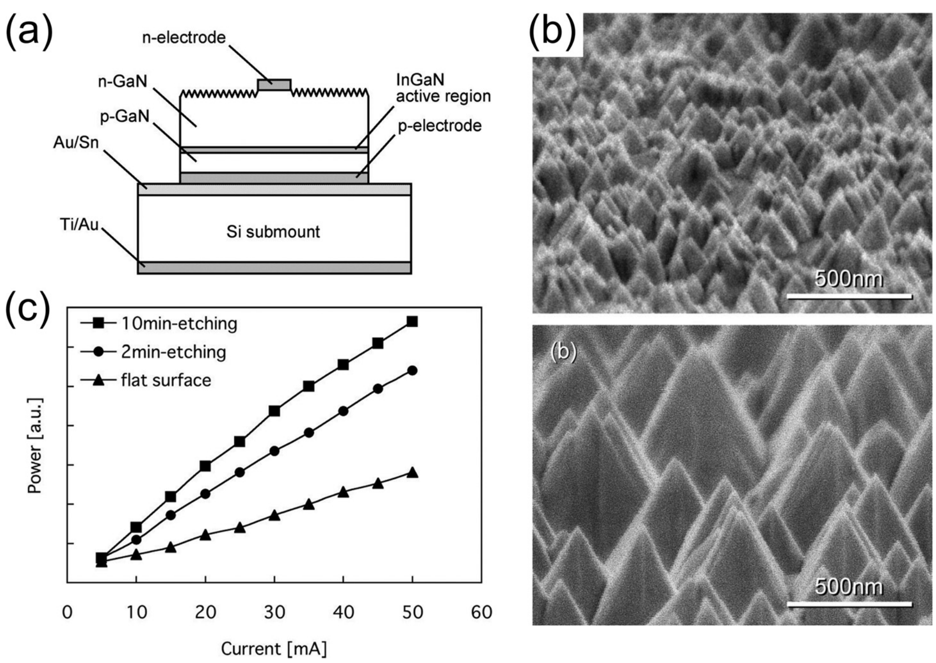

FIG. 11. (a) Schematic diagram of light emitting diode with surface roughening of nGaN. The nGaN is accessed using laser liftoff (LLO) technique and then flip-chip bonding it to a silicon substrate. (b) SEM images of the roughened nGaN surface etched by KOH-based photoelectrochemical method for 2 min etching and 10 min etching. (c) Output power is measured as a function of injected current. The 10-minute etch roughened surface LED showed a 2.3 times increase in the output power when compared to the flat surface LED. Reprinted with permission from Fujii *et al.*, Appl. Phys. Lett. **84**, 855 (2004).[165] Copyright 2004 American Institute of Physics.

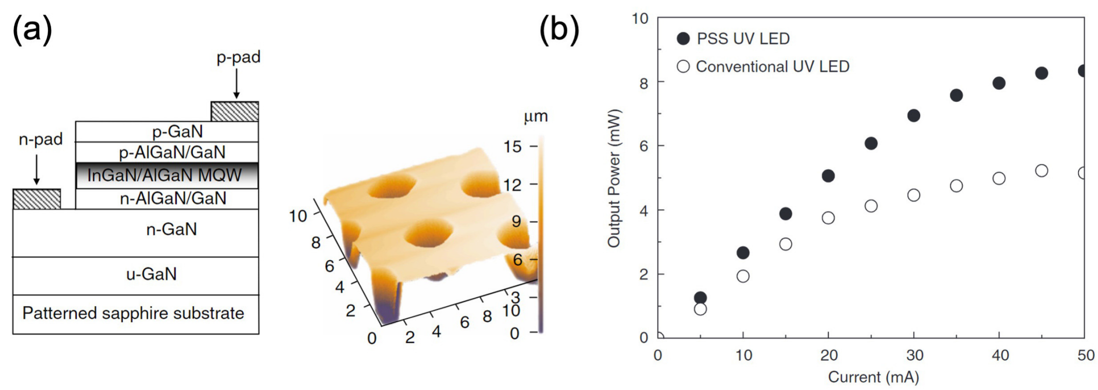

FIG. 12. Light emitting diode on a patterned sapphire substrate (a) A schematic diagram of UV-LED structure on a patterned sapphire substrate (PSS). The structure consists of u-GaN, n-GaN, multiple quantum wells (MQW) and p-GaN grown using metalorganic vapor phase epitaxy (MOVPE). An atomic force microscope (AFM) image of the bare PSS before MOVPE growth is also shown. (b) The output power of the UV-LED as a function of injected current density with PSS UV-LED and conventional UV-LED. PSS UV-LED shows higher output power at the same injected current than conventional LED. At 20 mA current operation, the output power increased from 3.75 to 5.06 mW, about 35% improvement. Reprinted with permission from Horng *et al.*, J. Crystal Growth **298**, 219 (2007).[182] Copyright 2006 Elsevier B.V.

VLC require a narrow beam of light as a source. The lower NA source is needed to prevent light leakage into adjacent pixels.[62,63] This section discusses methods for beam shaping, primarily focusing on microlenses and creating apertures on the top of the mesa structure of microLEDs.[186,187]

1. Microlens

Microlens arrays have been investigated for their focusing ability to achieve uniform far-field illumination of targets with laser beams in the past.[188] The microscale curved surface of the microlens allows it to focus divergent beamlets onto the illumination plane. Büttner *et al.* analyzed the beam shaping property of optical systems consisting of light-emitting diode and microlens arrays.[189] An integrated microlens array consisting of 128×96 elements at the bottom of a microLED array was shown to enable well-resolved light that prevented optical crosstalk.[190] The microlens was fabricated using a reflow method followed by etching the sapphire to transfer the pattern with an RMS roughness of less than 3 nm. Low roughness is needed for optically high-quality microlenses. Figures 13(a) and 13(b) show the schematic diagram of the integrated device and an image demonstrating the focusing ability of the microlens, respectively. Zhu *et al.* reported fabricating microlens arrays with UV-microLEDs as exposure sources. In far-field emissions measurements, the integrated device showed a significant reduction in light divergence.[186] The divergence half-angle was reduced by 22°.

The incorporation of silica/polystyrene (PS) colloidal microlens array on the top of microLEDs has been shown to increase light extraction at higher angular directions with increased PS thickness and to decrease divergence of light output at smaller PS thicknesses.[191] To further control beam shaping from light emitting diodes, an optical element combining a Fresnel lens with a microlens array design has been designed and studied for controlling on-axis and off-axis LED emission for lighting applications.[192] Continuing on the trend of integrating optical components with LEDs/microLEDs, a combination of total internal reflection (TIR) lenses, a reflective cavity, and a microlens array plate has been proposed for uniform street lighting using LEDs.[193]

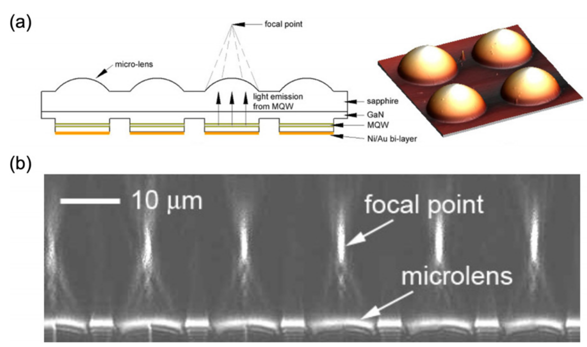

FIG. 13. Microlens integration with microLED. (a) Schematic diagram of an integrated device consisting of microLEDs and microlens arrays fabricated on the top of the sapphire substrate using photoresist reflow method followed by dry etching of the sapphire. It shows an AFM 3D image of the microlens of diameter 12 μm. (b) An image illustrating the focusing ability of the microlens using reflection/transmission confocal microscopic technique. The microlens has an approximate measured focal length of 8 μm and a center height of 1.8 μm. Reproduced with permission from Choi *et al.*, Phys. Status Solidi C **2**, 2903 (2005).[190] Copyright 2005 WILEY-VCH Verlag GmbH & Co. KGaA, Weinheim.

Additionally, Park *et al.* created a new type of compact optical element that combined a pair of microlens arrays for light collimation from micro-displays for the application of using microLEDs for near-eye displays.[194] Demory *et al.* demonstrated HWHM linewidth reduction of 50% in far-field emission divergence by integrating nearly flat parabolic nanolenses on the top of nanopillar microLEDs.[187] This demonstrates the potential for reducing the size and weight of collimation and projection optics by incorporating microlens arrays.

2. TIR Fresnel lens

A Fresnel lens is a compact lens that is made up of a set of concentric annular sections.[195] These sections can be viewed as divided surfaces of a standard lens with the same curvature and stepwise discontinuities between them. These lenses use refraction as well as a total internal reflection to achieve convergence, collimation, or divergence properties.[196] Parkyn *et al.* incorporated a TIR lens on light emitting diodes to achieve beam collimation for non-imaging devices.[197] Additionally, Chen *et al.* reported an optimized Fresnel lens for multiple LEDs to achieve uniform lighting for reading applications.[198] Other works have shown that Fresnel lenses can collimate LED light for fluorescence microscopy as well.[199]

Even though many applications of Fresnel lens with LEDs have been shown, a demonstration of its functionality for use with miniaturized optical components was missing. To close this gap, Joo *et al.* proposed a TIR Fresnel lens for a miniature electro-optical system that could collimate emitted light from LEDs more effectively.[200] The designed lens had a diameter of less than 1 mm and 11 facets on a single side. It successfully reduced the emission solid angle from 60° to 12°. Researchers have also investigated an electro-optical system that integrated a TIR Fresnel lens into the packaging microlens of LEDs, which can benefit systems that require focused and narrow microLED light emission.[201] The work explored the influence of structural parameters, namely, the height-to-width ratio of the 3D Fresnel-based lens, on beam shaping and showed improved narrowing of the emitted light beam.[201]

While a Fresnel lens is well-suited to collimate light sources, certain applications requiring uniform lighting from multiple light sources need further re-direction of the light beam.[192,193] Wang *et al.* proposed an optical element that combined a Fresnel lens and a microlens to achieve light collimation and further re-direction of collimated rays, respectively.[192] The proposed design method is versatile with no limitation on the source intensity pattern. The resulting optical element is compact and lightweight. A major challenge of creating optical systems that use a Fresnel lens for beam shaping is the mathematical complexity and intricate optimizations.[202,203] One proposed method tackles this issue by using geometric optics analysis to simplify the design process of a free-form lens system. The free-form lens consisted of a TIR collimator and Fresnel exit lens to produce specific LED intensity distribution.[204]

Another challenge for LEDs application is the limited optical power output from a single LED.[193] This requires using an array of LEDs/microLEDs to obtain higher optical power. These further need integration with an array of lens systems. Vu *et al.* presented a design for uniform lighting applications that consisted of a collimating plano–convex lens array and two perpendicularly-placed linear Fresnel lenses.[205] The physical layout of the illumination system and the simulation results showing uniform lighting is shown in Fig. 14. While the integration of TIR Fresnel lens systems and LEDs offers solutions to many of the challenges associated with beam shaping, the complex process of design and implementation significantly increases the cost of electro-optical systems. The addition of optical elements as a part of LED packaging can significantly address some of these challenges. A detailed review of the optical designs for the LED packaging by Nian *et al.* can be referred to for further insight.[206]

C. Wavelength management techniques

There are different techniques that are used to get multiple wavelength emissions from microLEDs. One of the most common methods is to change the material composition of the compound semiconductor layer. It is done by incorporating higher indium (In) content in the InGaN/GaN alloy which changes the crystal structure and eventually

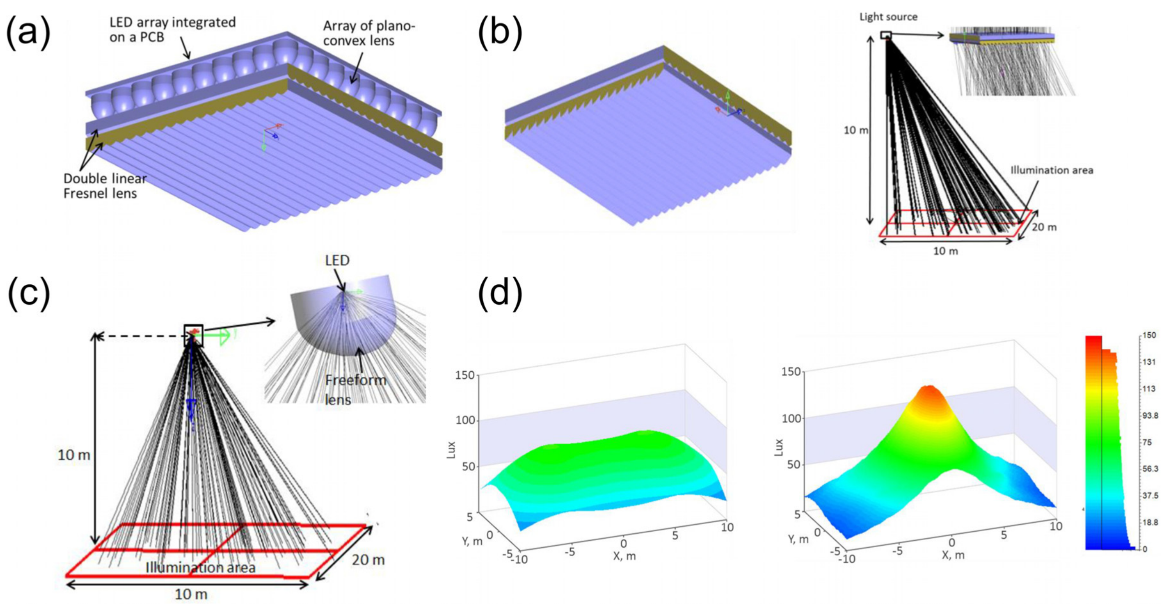

FIG. 14. Integration of Fresnel lens in an optical system to achieve uniform illumination. (a) The schematic layout of the illumination system consists of an LED array integrated on a PCB, an array of plano–convex lenses, and a double linear Fresnel lens array. (b) Ray-tracing simulation results of the proposed design with the double linear Fresnel lenses. The illumination area for simulation is $10 \times 20\ m^2$, and the light source is located at the height of 10 m. (c) Ray-tracing simulation of an illumination system with a freeform optics design. The illumination area for simulation is $10 \times 20\ m^2$, and the light source is located at the height of 10 m in the center. (d) Light intensity distribution comparison of the LED illumination system with Fresnel lens and freeform optics system. A more uniform light intensity distribution is achieved using the double Fresnel lenses system. Reproduced reprinted with permission from Vu *et al.*, Energies **10**, 2091 (2017).[205] Copyright 2017, Authors, licensed under a Creative Common CC BY 4.0 license.

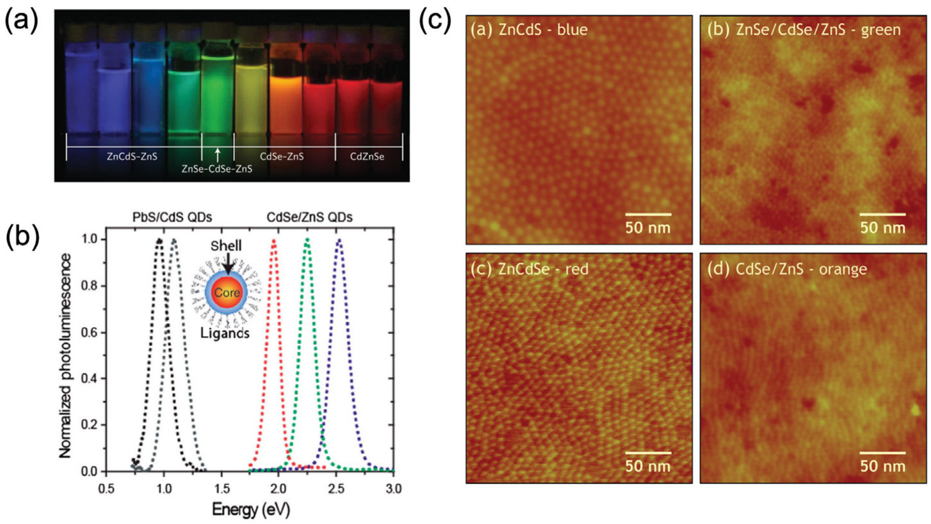

FIG. 15. (a) Various QDs in chloroform solutions showing photoluminescence under UV light with emission centered around 365 nm. (b) Photoluminescence spectra of CdSe/ZnS and PbS/CdS core/shell colloidal QDs. The inset shows the schematic of QDs with core, shell, and ligands attached. The spectra show the narrowband emission from visible into near-IR. Reproduced with permission from V. Wood and V. Bulović, Nano Rev. **1**, 5202 (2010).[215] Copyright 2010 Authors, licensed under a Creative Commons Attribution-Noncommercial 3.0 Unported License. (c) AFM height images of various QDs showing close-packed monolayers. (a) and (c) reprinted with permission from Anikeeva *et al.*, Nano Lett. **9**, 2532 (2009).[221] Copyright 2009 American Chemical Society.

modifies the bandgap of the semiconductor. In addition to modifying the lattice constant of the material, adding quantum dots (QD) or phosphors to the mesa surface of microLEDs could enable a single-colored pixel to emit multiple colors.[207,208] All three methods to achieve different wavelength emissions are discussed in this section. Other techniques such as quantum well (QW) thickness-dependent InGaN/GaN multiple quantum wells (MQW), microfacet emission from MQW, nanowires, and local strain engineering have also been explored in the literature for wavelength tuning in microLEDs.[209–213]

1. Colloidal Quantum Dots (QDs)

QDs are nanoscale semiconductor crystals with distinct properties from those of bulk semiconductors.[214,215] Each QD consists of a small inorganic semiconductor core (1–10 nm), a wider-bandgap semiconductor shell, and a coating of passivating ligands.[216,217] An atomic force microscopy (AFM) height image of a closely packed monolayer of QDs is shown in Fig. 15(c). One of the most useful properties of these nanocrystals is the tunability of their bandgap by varying their size and discrete energy levels also called the quantum confined effect.[215,218] Figure 15(a) shows QD solutions of various sizes and composition exhibiting photoluminescence under UV light. Figure 15(b) shows the PL spectra of QDs with narrowband emission from visible to NIR. Several advantageous properties of QDs such as narrow emission linewidth (20–30 nm for CdSe), high photoluminescence quantum yield (PLQY > 90%), high photostability, and solution processability make them attractive for applications with microLEDs.[126,219] CdSe, with an emission linewidth of 20–30 nm, and PbS are the most commonly used materials for the core of the QDs for visible wavelength and NIR devices, respectively.[214,220,221]

As mentioned in the application section, microLEDs are used in VLC systems to achieve higher bandwidth and data transfer speeds. This has motivated the adoption of white light microLEDs with larger pixel sizes of 100 μm into VLC systems to achieve higher data transfer rates without complicated signal processing.[120] As a result, it has become essential to find a white light source with wavelength multiplexing ability for VLC systems. Recently, researchers have explored QD-based white light microLEDs for VLC applications. Mei *et al.* demonstrated a white light system that used Perovskite QDs for a high bandwidth VLC system.[124] They showed $80 \times 80\,\mu m^2$ microLEDs having a modulation bandwidth of 160 MHz and a peak emission wavelength of approximately 445 nm. They achieve bandwidths of up to 85 MHz without filters or equalization in the white-light system. The system showed a maximum data transfer rate of 300 Mbps using a non-return-to-zero on-off keying (NRZ-OOK) modulation scheme. QD-based microLED arrays for bi-directional optogenetics applications have also been reported.[222] They used QDs to create a dual-colored microLED array with emissions at 462 and 623 nm. This further elucidates the use of QDs in non-display application technologies.

2. Phosphor

Phosphors are color-converting materials that are essential for achieving full color and are a key component of white lighting systems.[5,223,224] Generally, phosphors consist of two functional materials, a host material, and an activator material.[225] Host materials are often wide bandgap oxides, nitrides, or sulfides and determine the crystal structure of the phosphor.[226–228] Activator materials are usually transition metals or rare earth compounds and are responsible for light emission.[225] Both materials play critical roles in determining a phosphor's photoluminescent properties, such as emission wavelength and quantum efficiency. Figure 16(a) shows the crystal structure of a narrowband red-emitting phosphor material $Sr_4[LiAl_{11}N_{14}]:Eu^{2+}$ as an example.[229]

Traditionally, phosphors have been a preferred choice as a down-conversion material for UV-LEDs and blue LEDs to obtain white light sources, due to their high efficiency, high stability, and narrow spectrum.[125,229,230] However, phosphors' larger size can cause significant non-uniformity in the color conversion when used with small (50 μm) microLEDs. The size of the phosphor can be varied depending upon the preparation process and nano-sized phosphors can be prepared.[231] However, the luminous efficiency of the phosphor is proportional to its size, and as a result, nano-sized phosphors have lower luminous efficiencies.[232]

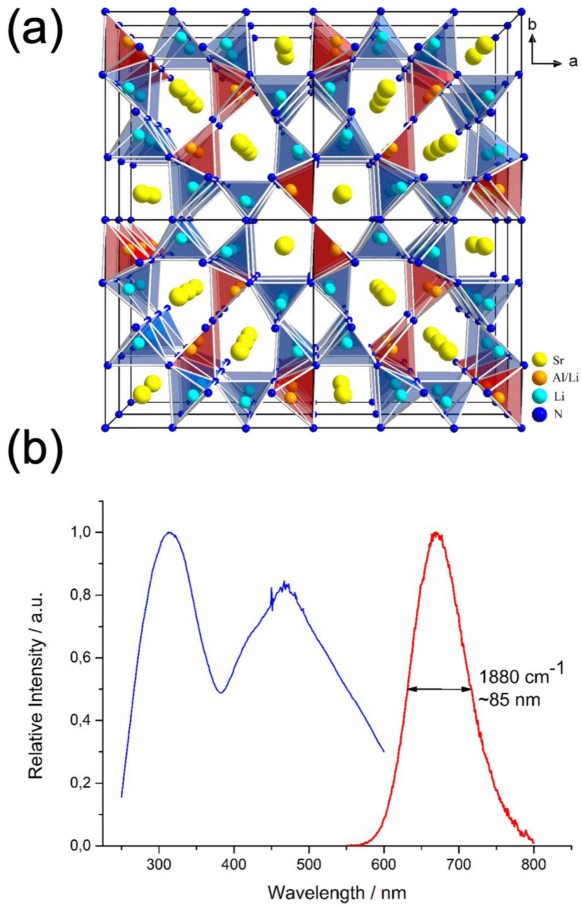

FIG. 16. Phosphor structure and emission spectrum. (a) The crystal structure of a narrowband red-emitting phosphor material $Sr_4[LiAl_{11}N_{14}]:Eu^{2+}$ along [001] direction. The nitride is the host material responsible for the crystal structure. The rare earth metal Eu^{2+} is the activator material responsible for light emission. (b) Excitation (peak at 460 nm) and emission spectra of the phosphor $Sr_4[LiAl_{11}N_{14}]:Eu^{2+}$. It shows red luminescence with an emission peak at 670 nm and a bandwidth of 85 nm. Reprinted with permission from Wilhelm *et al.*, Chem. Mater. **29**, 1204 (2017).[229] Copyright 2009 American Chemical Society.

Phosphors integrated with blue microLEDs for VLC communication have been reported. Chun *et al.* presented a high-speed VLC system with a transmission rate of 1.68 Gbps at a distance of 3 cm using white light generated by blue GaN microLEDs and a yellow fluorescent converter.[123] The high transmission speed is attributed to the high modulation bandwidth of the polymer-based yellow fluorescent layer. Huang *et al.* reported a white light VLC system with a 3-dB modulation bandwidth of 127.3 MHz using blue microLEDs and yellow phosphor.[122] Recently, Chang *et al.* reported a white light VLC system that used semi-polar blue microLEDs and yellow phosphors to achieve a data rate of 2.805 Gbps.[128] The higher data rate and bandwidth of the system are attributed to the improved radiative efficiency of the semi-polar blue microLEDs resulting from the reduced quantum-confined Stark effect (QCSE).

A hybrid strategy of mixing small-sized and large-sized phosphors can improve the non-uniformity of the system to a great extent with only a small reduction in efficiency. However, this remains a challenge as mesa dimensions shrink to smaller areas of 5 μ m and below.[204] Recently, GE has developed a sub-micron sized red phosphor $K_2SiF_6:Mn^{4+}$ (KSF) and KSF inks suitable for microLEDs that can be deposited by low-cost methods such as ink-jet printing, slot die coating, or spin coating.[233] These recent developments pave the way for phosphors to be further utilized in microLED applications by overcoming challenges due to their size.

3. Compound semiconductor layers

Electroluminescence, which is responsible for spontaneous light emission upon the passage of electric current, dates back to 1907 when Round discovered it in silicon carbide (SiC) crystals.[234] Further understanding of materials and luminescent phenomena makes tuning of bandgap an obvious choice for the creation of light emitting diodes of different colors.[235–238] Red LEDs have traditionally used AlGaInP crystals, but recent focus has shifted to indium gallium nitride (InGaN) crystals as they offer a wide spectral range from ultraviolet to infrared.[239] InGaN bandgap energy can be tuned from 0.67 to 3.42 eV by changing the composition of the alloy.[129,240,241] Figure 17 shows the energy bandgap of hexagonal gallium nitride (h-GaN) as a function of lattice constant that is controlled by the indium (In) concentration in the alloy.

The external quantum efficiency (EQE) of the microLED decreases with decreasing device size due to the increased non-radiative recombination, also known as efficiency droop.[100] While the peak EQE of a 20 × 20 μm blue microLED has been reported to be as high as 33%, AlGaInP-based red microLEDs suffer significantly from efficiency droop due to high surface recombination and long carrier lifetime at smaller dimensions (<50 μm).[242–244] They also suffer from poor thermal stability at high temperatures.[245,246] This has resulted in a growing interest in creating red microLEDs that are based on III-nitride materials, in particular InGaN.[247,248] The EQE of red InGaN

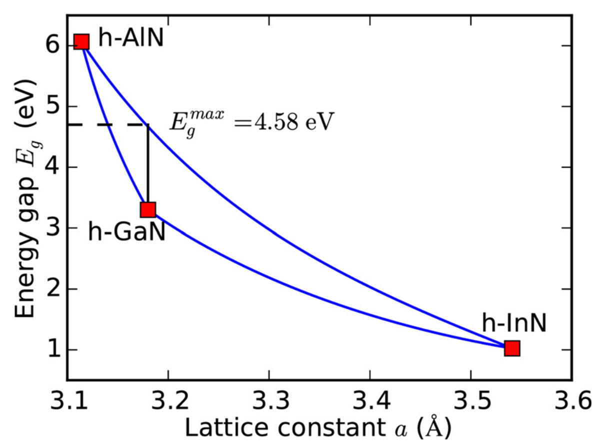

FIG. 17. The plot of energy bandgap vs lattice constant for hexagonal III-nitride alloys. The energy bandgap of the h-GaN changes from 3.42 to 0.67 eV as the indium content increases in the alloy. This changes the lattice constant of InGaN crystal from approximately 3.18 – 3.55 Å. Reproduced with permission from Freitas *et al.*, AIP Adv. **6**, 085308 (2016). Copyright 2016, Authors, licensed under a Creative Commons Attribution (CC BY) License.[239]

microLEDs is still notably low because increasing indium (In) content in the alloy degrades crystal quality due to a large lattice mismatch and low-temperature growth.[249] Various fabrication techniques, such as strain engineering, lower growth rates, and high growth temperatures, are required to tackle the low EQE problem facing III-nitride based red microLEDs.[250] A more detailed review of the development of red microLEDs can be found in the manuscript from Iida *et al.*[250]

Apart from applications in display technologies, the development of different colored efficient microLEDs is important for other applications such as optogenetics. The activation or suppression of different cells expressed by different proteins is highly desirable for more precise control over the neuronal activity. Red-and-blue-colored microLED-based optoelectronic probes have been used to demonstrate bi-directional neuronal activity manipulation.[251,252] Dual-colored microLED arrays have also been used as VLC transmitters and demonstrated error-free data rates of 1.79–3.35 Gbps in a dual-wavelength multiplexing scheme.[253] Further work is needed to enhance the efficiency of longer wavelength microLEDs as longer wavelengths enable deeper neural cell stimulation in optogenetics and wavelength division multiplexing in VLC systems.[254,255]

V. OUTLOOK AND CHALLENGES

As discussed in the article, MicroLED/LED technology has been incorporated into a range of applications beyond display applications. MicroLEDs based on InGaN/GaN have consistently higher efficiencies than competing approaches even as we scale down the device dimensions to sub-micron size for blue, green, and red emissions. The efficiency of the red-colored InGaN/GaN microLEDs can stand further improvement, especially at smaller dimensions. The ability to achieve RGB emission from a single material stack will open a wide array of applications with increasingly complex system integration. Additionally, the relatively high cost of GaN epi wafers remains a challenge to be addressed, as microLED technology is adopted into a greater number of applications such as point-of-care medical applications like phototherapy and skin treatments.[256,257]

The adoption of microLEDs in visible light communication (VLC) systems has rapidly grown with improved data transfer rates. An increase in the modulation bandwidth is the driving factor for the higher data transfer rates. Device miniaturization and the decrease in carrier lifetime of microLEDs can further improve this trend. Additionally, VLC systems that use an array of microLEDs as emitters have the potential to enhance the data transfer rates even higher, albeit with the increased system complexity. Implementation of VLC in laboratory setup is routinely demonstrated, but the real-life system still remains a challenge. Many critical issues such as reliability, scalability, and compactness related to the commercialization of the VLC systems remain to be addressed.

As optogenetics advances our understanding of neural circuits, microLEDs will have an increasingly prevalent role in delivering spatially resolved single-neuron stimulation. This would require scaling down microLEDs further along and improving external efficiency to be able to deliver enough light irradiation to create action potentials. The mesa size-related efficiency droop needs to be further improved. Closed loop stimulation and monitoring of a large ensemble of neurons would require large-scale device fabrication. Integration with microLED drivers and electrode arrays also needs to be addressed. As microLEDs are scaled down to the nanoscale, they will have the potential for an entirely new concept of microscopy, NIM with resolution capabilities surpassing the diffraction limit. However, as the microLEDs are miniaturized to nanoscale dimensions, increased non-radiative recombination due to the larger surface-to-volume ratio of the mesa becomes a challenge.[15,16] Various mesa sidewall passivation methods, such as dielectric (e.g., SiO_2, Al_2O_3) deposition using plasma-enhanced chemical vapor deposition (PECVD) and atomic layer deposition (ALD), acid-base etching, hydrogen plasma, and sulfur treatments, are suggested ways to minimize non-radiative recombination and improve the external quantum efficiency.[258–261]

Progress toward improving the extraction efficiency of LEDs using photonic crystals and beam shaping using microlenses has been made, but challenges related to reliable integration with microLEDs remain to be addressed. The most common microlens fabrication technique (as the reflow method) faces uniformity and control challenges that need to be improved. The fabrication of high-quality optical microlenses to minimize scattering is also a challenge. Photonic crystal fabrication often requires using electron beam lithography which is expensive and offers a low throughput. Simpler and more reliable fabrication techniques need to be developed for further integration with microLEDs and to enable more widespread utilization of these advanced methods.

The ability to modify the electro-optical properties of microLEDs using various techniques has the potential to enable even more applications beyond displays. MicroLEDs can be used further as active elements in chemical sensors for environmental monitoring and optically activating gas sensors to enable room temperature gas sensing.[262–264] The potential of microLEDs as a light source for various computational microscopy techniques further remains to be explored. More research into eliminating size-scaling related efficiency droop as well as compatibility and integration with silicon processing needs to be undertaken to further reduce cost and improve integration. These advances will give a much-needed boost to the InGaN/GaN based microLED technology and help develop additional applications with the potential to be ubiquitous in everyday life.

ACKNOWLEDGMENTS

The authors acknowledge funding support from the National Institutes of Health (NIH) through Grant No. 1R01NS123665 and NSF Grant No. 1926676. Vikrant Kumar would like to thank Dr. Christine McGinn, Dr. Keith Behrman, Megan Noga, Oliver Durnan, and Zicong Huang for their editing and valuable suggestions in the manuscript preparation.

AUTHOR DECLARATIONS

Conflict of Interest

Yes, I.K. is a co-founder of Lumiode, which is a company working in microLED displays and holds an equity stake in the company. V.K. has no competing financial interest.

Author Contributions

Vikrant Kumar: Conceptualization (equal); Visualization (lead); Writing – original draft (lead); Writing – review & editing (lead). **Ioannis Kymissis:** Conceptualization (equal); Funding acquisition (lead); Supervision (lead); Writing – review & editing (supporting).

DATA AVAILABILITY

The data that support the findings of this study are available within the article.

REFERENCES

[1]S. Nakamura and M. R. Krames, "History of gallium-nitride-based light-emitting diodes for illumination," Proc. IEEE **101**, 2211–2220 (2013).
[2]J. Cho, J. H. Park, J. K. Kim, and E. F. Schubert, "White light-emitting diodes: History, progress, and future," Laser Photonics Rev. **11**, 1600147 (2017).
[3]S. P. Denbaars, D. Feezell, K. Kelchner, S. Pimputkar, C. C. Pan, C. C. Yen, S. Tanaka, Y. Zhao, N. Pfaff, R. Farrell, M. Iza, S. Keller, U. Mishra, J. S. Speck, and S. Nakamura, "Development of gallium-nitride-based light-emitting diodes (LEDs) and laser diodes for energy-efficient lighting and displays," Acta Mater. **61**, 945–951 (2013).
[4]S. Nakamura, "Nobel Lecture: Background story of the invention of efficient blue InGaN light emitting diodes," Rev. Mod. Phys. **87**, 1139 (2015).
[5]R. Mueller-Mach, G. O. Mueller, M. R. Krames, and T. Trottier, "High-power phosphor-converted light-emitting diodes based on III-nitrides," IEEE J. Sel. Top. Quantum Electron. **8**, 339–345 (2002).
[6]G. Li, W. Wang, W. Yang, Y. Lin, H. Wang, Z. Lin, and S. Zhou, "GaN-based light-emitting diodes on various substrates: A critical review," Rep. Prog. Phys. **79**, 056501 (2016).
[7]H. S. El-Ghoroury, M. Yeh, J. C. Chen, X. Li, and C. L. Chuang, "Growth of monolithic full-color GaN-based LED with intermediate carrier blocking layers," AIP Adv. **6**, 075316 (2016).
[8]K. Kishino, K. Nagashima, and K. Yamano, "Monolithic integration of InGaN-based nanocolumn light-emitting diodes with different emission colors," Appl. Phys. Express **6**, 012101 (2013).
[9]H. S. El-Ghoroury, C.-L. Chuang, and M. V. Kisin, "III-nitride monolithic LED covering full RGB color gamut," Proc. SPIE **9742**, 974222 (2016).
[10]A. Rehman Anwar, M. T. Sajjad, M. Ali Johar, C. A. Hernández-Gutiérrez, M. Usman, and S. P. Łepkowski, "Recent progress in micro-LED-based display technologies," Laser Photonics Rev. **16**, 2100427 (2022).
[11]Y. Wu, J. Ma, P. Su, L. Zhang, and B. Xia, "Full-color realization of micro-LED displays," Nanomaterials **10**, 1–33 (2020).
[12]See https://www.ledinside.com/showreport/2020/1/ces2020_microled_japan-korea for C. Yining, "CES 2020: Multi-size Micro LED displays revealed by Japan and Korea Tech Giants—LEDinside," (2020).
[13]See https://www.roadtovr.com/ces-2020-jbd-micro-led-ar-vr-absurd-brightness/ for L. Ben, "CES 2020: JBD micro LED display for AR/VR with 3 Million Nits brightness," (2020).
[14]See https://www.ledinside.com/node/31245 for C. Yining, "Compound Photonics Releases World's Smallest Optical Engine for Micro LED Smart Glasses—LEDinside," (2020).
[15]S. L. Chen, W. M. Chen, F. Ishikawa, and I. A. Buyanova, "Suppression of non-radiative surface recombination by n incorporation in GaAs/GaNAs core/shell nanowires," Sci. Rep. **5**, 11653 (2015).
[16]A. Daami, F. Olivier, L. Dupré, F. Henry, and F. Templier, "59–4: *Invited paper:* Electro-optical size-dependence investigation in GaN micro-LED devices," in *SID Symposium—Digest of Technical Papers* (Wiley Online Library, 2018), Vol. 49, pp. 790–793.
[17]W. Tian and J. Li, "Size-dependent optical-electrical characteristics of blue GaN/InGaN micro-light-emitting diodes," Appl. Opt. **59**, 9225–9232 (2020).
[18]K. Behrman and I. Kymissis, "Enhanced microLED efficiency via strategic pGaN contact geometries," Opt. Express **29**, 14841–14852 (2021).
[19]J. J. D. McKendry, R. P. Green, A. E. Kelly, Z. Gong, B. Guilhabert, D. Massoubre, E. Gu, and M. D. Dawson, "High-speed visible light communications using individual pixels in a micro light-emitting diode array," IEEE Photonics Technol. Lett. **22**, 1346–1348 (2010).
[20]P. Tian, X. Liu, S. Yi, Y. Huang, S. Zhang, X. Zhou, L. Hu, L. Zheng, and R. Liu, "High-speed underwater optical wireless communication using a blue GaN-based micro-LED," Opt. Express **25**, 1193–1201 (2017).
[21]X. Liu, R. Lin, H. Chen, S. Zhang, Z. Qian, G. Zhou, X. Chen, X. Zhou, L. Zheng, R. Liu, and P. Tian, "High-bandwidth InGaN self-powered detector arrays toward MIMO visible light communication based on micro-LED arrays," ACS Photonics **6**, 3186–3195 (2019).
[22]V. Poher, N. Grossman, G. T. Kennedy, K. Nikolic, H. X. Zhang, Z. Gong, E. M. Drakakis, E. Gu, M. D. Dawson, P. M. W. French, P. Degenaar, and M. A. A. Neil, "Micro-LED arrays: A tool for two-dimensional neuron stimulation," J. Phys. D **41**, 094014 (2008).
[23]S. E. Mondello, B. D. Pedigo, M. D. Sunshine, A. E. Fischedick, P. J. Horner, and C. T. Moritz, "A micro-LED implant and technique for optogenetic stimulation of the rat spinal cord," Exp. Neurol. **335**, 113480 (2021).
[24]F. Michoud, C. Seehus, P. Schönle, N. Brun, D. Taub, Z. Zhang, A. Jain, I. Furfaro, O. Akouissi, R. Moon *et al.*, "Epineural optogenetic activation of nociceptors initiates and amplifies inflammation," Nat. Biotechnol. **39**, 179–185 (2021).
[25]V. Poher, H. X. Zhang, G. T. Kennedy, C. Griffin, S. Oddos, E. Gu, D. S. Elson, J. M. Girkin, P. M. W. French, M. D. Dawson, and M. A. A. Neil, "Optical sectioning microscopes with no moving parts using a micro-stripe array light emitting diode," Opt. Express **15**, 11196–11206 (2007).
[26]D. Dan, M. Lei, B. Yao, W. Wang, M. Winterhalder, A. Zumbusch, Y. Qi, L. Xia, S. Yan, Y. Yang, P. Gao, T. Ye, and W. Zhao, "DMD-based LED-illumination super-resolution and optical sectioning microscopy," Sci. Rep. **3**, 1116 (2013).
[27]D. Elfström, B. Guilhabert, J. Mckendry, S. Poland, Z. Gong, D. Massoubre, E. Richardson, B. R. Rae, G. Valentine, G. Blanco-Gomez, E. Gu, J. M. Cooper, R. K. Henderson, and M. D. Dawson, "Mask-less ultraviolet photolithography based on CMOS-driven micro-pixel light emitting diodes," Opt. Express **17**, 23522–23529 (2009).
[28]B. R. Tull, Z. Basaran, D. Gidony, A. B. Limanov, J. S. Im, I. Kymissis, and V. W. Lee, "26.2: Invited paper: High brightness, emissive microdisplay by integration of III-V leds with thin film silicon transistors," in *SID Symposium Digest of Technical Papers* (Wiley Online Library, 2015), Vol. 46, pp. 375–377.
[29]F. Templier, "GaN-based emissive microdisplays: A very promising technology for compact, ultra-high brightness display systems," J. Soc. Inf. Disp. **24**, 669–675 (2016).
[30]Y. Huang, G. Tan, F. Gou, M. C. Li, S. L. Lee, and S. T. Wu, "Prospects and challenges of mini-LED and micro-LED displays," J. Soc. Inf. Disp. **27**, 387–401 (2019).
[31]T. Wu, C. W. Sher, Y. Lin, C. F. Lee, S. Liang, Y. Lu, S. W. H. Chen, W. Guo, H. C. Kuo, and Z. Chen, "Mini-LED and Micro-LED: Promising candidates for the next generation display technology," Appl. Sci. **8**, 1557 (2018).
[32]L. Chaudet, M. Neil, P. Degenaar, K. Mehran, R. Berlinguer-Palmini, B. Corbet, P. Maaskant, D. Rogerson, P. Lanigan, E. Bamberg, and B. Roska, "Development of optics with micro-LED arrays for improved opto-electronic neural stimulation," Optogenetics **8586**, 85860R (2013).
[33]C. W. Jeon, E. Gu, and M. D. Dawson, "Mask-free photolithographic exposure using a matrix-addressable micropixellated AlInGaN ultraviolet light-emitting diode," Appl. Phys. Lett. **86**, 221105 (2005).
[34]C. Yang, S. P. Turaga, A. A. Bettiol, P. Balamuniappan, M. Bosman, H. R. Tan, J. H. Teng, and E. J. Teo, "Textured V-pit green light emitting diode as a wavelength-selective photodetector for fast phosphor-based white light modulation," ACS Photonics **4**, 443–448 (2017).
[35]S. W. H. Chen, Y. M. Huang, Y. H. Chang, Y. Lin, F. J. Liou, Y. C. Hsu, J. Song, J. Choi, C. W. Chow, C. C. Lin, R. H. Horng, Z. Chen, J. Han, T. Wu, and H. C. Kuo, "High-bandwidth green semipolar (20–21) InGaN/GaN micro light-emitting diodes for visible light communication," ACS Photonics **7**, 2228–2235 (2020).
[36]A. Rashidi, M. Nami, M. Monavarian, A. Aragon, K. Davico, F. Ayoub, S. Mishkat-Ul-Masabih, A. Rishinaramangalam, and D. Feezell, "Differential carrier lifetime and transport effects in electrically injected III-nitride light-emitting diodes," J. Appl. Phys. **122**, 035706 (2017).
[37]J. J. D. McKendry, D. Massoubre, S. Zhang, B. R. Rae, R. P. Green, E. Gu, R. K. Henderson, A. E. Kelly, and M. D. Dawson, "Visible-light communications using a CMOS-controlled micro-light-emitting-diode array," J. Lightwave Technol. **30**, 61–67 (2012).
[38]E. Xie, R. Bian, X. He, M. S. Islim, C. Chen, J. J. D. Mckendry, E. Gu, H. Haas, and M. D. Dawson, "Over 10 Gbps VLC for long-distance applications using a GaN-based series-biased micro-LED array," IEEE Photonics Technol. Lett. **32**, 499–502 (2020).

[39]N. Chi, *LED-Based Visible Light Communications*, 1st ed. (Springer Berlin, Heidelberg, 2018).
[40]E. S. Boyden, F. Zhang, E. Bamberg, G. Nagel, and K. Deisseroth, "Millisecond-timescale, genetically targeted optical control of neural activity," Nat. Neurosci. **8**, 1263–1268 (2005).
[41]K. Deisseroth, G. Feng, A. K. Majewska, G. Miesenböck, A. Ting, and M. J. Schnitzer, "Next-generation optical technologies for illuminating genetically targeted brain circuits," J. Neurosci. **26**, 10380–10386 (2006).
[42]F. Zhang, L. P. Wang, E. S. Boyden, and K. Deisseroth, "Channelrhodopsin-2 and optical control of excitable cells," Nat. Methods **3**, 785–792 (2006).
[43]V. Gradinaru, K. R. Thompson, F. Zhang, M. Mogri, K. Kay, M. B. Schneider, and K. Deisseroth, "Targeting and readout strategies for fast optical neural control *in vitro* and *in vivo*," J. Neurosci. **27**, 14231–14238 (2007).
[44]L. A. Gunaydin, O. Yizhar, A. Berndt, V. S. Sohal, K. Deisseroth, and P. Hegemann, "Ultrafast optogenetic control," Nat. Neurosci. **13**, 387–392 (2010).
[45]L. Fenno, O. Yizhar, and K. Deisseroth, "The development and application of optogenetics," Annu. Rev. Neurosci. **34**, 389–412 (2011).
[46]E. S. Boyden, "Optogenetics and the future of neuroscience," Nat. Neurosci. **18**, 1200–1201 (2015).
[47]X. Xu, T. Mee, and X. Jia, "New era of optogenetics: From the central to peripheral nervous system," Crit. Rev. Biochem. Mol. Biol. **55**, 1–16 (2020).
[48]A. M. Aravanis, L. P. Wang, F. Zhang, L. A. Meltzer, M. Z. Mogri, M. B. Schneider, and K. Deisseroth, "An optical neural interface: *In vivo* control of rodent motor cortex with integrated fiberoptic and optogenetic technology," J. Neural Eng. **4**, S143 (2007).
[49]F. Wu, E. Stark, M. Im, I. J. Cho, E. S. Yoon, G. Buzsáki, K. D. Wise, and E. Yoon, "An implantable neural probe with monolithically integrated dielectric waveguide and recording electrodes for optogenetics applications," J. Neural Eng. **10**, 056012 (2013).
[50]N. McAlinden, D. Massoubre, E. Richardson, E. Gu, S. Sakata, M. D. Dawson, and K. Mathieson, "Thermal and optical characterization of micro-LED probes for *in vivo* optogenetic neural stimulation," Opt. Lett. **38**, 992 (2013).
[51]S. Dufour and Y. De Koninck, "Optrodes for combined optogenetics and electrophysiology in live animals," Neurophotonics **2**, 031205 (2015).
[52]N. Grossman, V. Poher, M. S. Grubb, G. T. Kennedy, K. Nikolic, B. McGovern, R. B. Palmini, Z. Gong, E. M. Drakakis, M. A. A. Neil, M. D. Dawson, J. Burrone, and P. Degenaar, "Multi-site optical excitation using ChR2 and micro-LED array," J. Neural Eng. **7**, 016004 (2010).
[53]F. Wu, E. Stark, P. C. Ku, K. D. Wise, G. Buzsáki, and E. Yoon, "Monolithically integrated μLEDs on silicon neural probes for high-resolution optogenetic studies in behaving animals," Neuron **88**, 1136–1148 (2015).
[54]R. Scharf, T. Tsunematsu, N. McAlinden, M. D. Dawson, S. Sakata, and K. Mathieson, "Depth-specific optogenetic control *in vivo* with a scalable, high-density μLED neural probe," Sci. Rep. **6**, 28381 (2016).
[55]B. Ji, Z. Guo, M. Wang, B. Yang, X. Wang, W. Li, and J. Liu, "Flexible polyimide-based hybrid opto-electric neural interface with 16 channels of micro-LEDs and electrodes," Microsyst. Nanoeng. **4**, 27 (2018).
[56]N. McAlinden, Y. Cheng, R. Scharf, E. Xie, E. Gu, C. F. Reiche, R. Sharma, P. Tathireddy, P. Tathireddy, L. Rieth, S. Blair, and K. Mathieson, "Multisite microLED optrode array for neural interfacing," Neurophotonics **6**, 035010 (2019).
[57]C. Liu, Y. Zhao, X. Cai, Y. Xie, T. Wang, D. Cheng, L. Li, R. Li, Y. Deng, H. Ding, G. Lv, G. Zhao, L. Liu, G. Zou, M. Feng, Q. Sun, L. Yin, and X. Sheng, "A wireless, implantable optoelectrochemical probe for optogenetic stimulation and dopamine detection," Microsyst. Nanoeng. **6**, 64 (2020).
[58]K. Kim, M. Vöröslakos, J. P. Seymour, K. D. Wise, G. Buzsáki, and E. Yoon, "Artifact-free and high-temporal-resolution in vivo opto-electrophysiology with microLED optoelectrodes," Nat. Commun. **11**, 2063 (2020).
[59]A. G. York, S. H. Parekh, D. D. Nogare, R. S. Fischer, K. Temprine, M. Mione, A. B. Chitnis, C. A. Combs, and H. Shroff, "Resolution doubling in live, multicellular organisms via multifocal structured illumination microscopy," Nat. Methods **9**, 749–754 (2012).
[60]D. J. Cai, D. Aharoni, T. Shuman, J. Shobe, J. Biane, W. Song, B. Wei, M. Veshkini, M. La-Vu, J. Lou, S. E. Flores, I. Kim, Y. Sano, M. Zhou, K. Baumgaertel, A. Lavi, M. Kamata, M. Tuszynski, M. Mayford, P. Golshani, and A. J. Silva, "A shared neural ensemble links distinct contextual memories encoded close in time," Nature **534**, 115–118 (2016).
[61]O. Skocek, T. Nöbauer, L. Weilguny, F. Martínez Traub, C. N. Xia, M. I. Molodtsov, A. Grama, M. Yamagata, D. Aharoni, D. D. Cox, P. Golshani, and A. Vaziri, "High-speed volumetric imaging of neuronal activity in freely moving rodents," Nat. Methods **15**, 429–432 (2018).
[62]K. Yanny, N. Antipa, W. Liberti, S. Dehaeck, K. Monakhova, F. L. Liu, K. Shen, R. Ng, and L. Waller, "Miniscope3D: Optimized single-shot miniature 3D fluorescence microscopy," Light **9**, 171 (2020).
[63]O. D. Supekar, A. Sias, S. R. Hansen, G. Martinez, G. C. Peet, X. Peng, V. M. Bright, E. G. Hughes, D. Restrepo, D. P. Shepherd, C. G. Welle, J. T. Gopinath, and E. A. Gibson, "Miniature structured illumination microscope for *in vivo* 3D imaging of brain structures with optical sectioning," Biomed. Opt. Express **13**, 2530 (2022).
[64]M. A. A. Neil, R. Juškaitis, and T. Wilson, "Method of obtaining optical sectioning by using structured light in a conventional microscope," Opt. Lett. **22**, 1905–1907 (1997).
[65]M. G. L. Gustafsson, "Surpassing the lateral resolution limit by a factor of two using structured illumination microscopy," J. Microsc. **198**, 82–87 (2000).
[66]T. Fukano and A. Miyawaki, "Whole-field fluorescence microscope with digital micromirror device: Imaging of biological samples," Appl. Opt. **42**, 4119–4124 (2003).
[67]A. A. Adeyemi, N. Barakat, and T. E. Darcie, "Applications of digital micromirror devices to digital optical microscope dynamic range enhancement," Opt. Express **17**, 1831–1843 (2009).
[68]A. Masson, M. Pedrazzani, S. Benrezzak, P. Tchenio, T. Preat, and D. Nutarelli, "Micromirror structured illumination microscope for high-speed in vivo drosophila brain imaging," Opt. Express **22**, 1243 (2014).
[69]A. Sandmeyer, M. Lachetta, H. Sandmeyer, W. Hübner, T. Huser, and M. Müller, "DMD-based super-resolution structured illumination microscopy visualizes live cell dynamics at high speed and low cost," bioRxiv 797670 (2019).
[70]M. Li, Y. Li, W. Liu, A. Lal, S. Jiang, D. Jin, H. Yang, S. Wang, K. Zhanghao, and P. Xi, "Structured illumination microscopy using digital micro-mirror device and coherent light source," Appl. Phys. Lett. **116**, 233702 (2019).
[71]D. Dan, B. Yao, and M. Lei, "Structured illumination microscopy for super-resolution and optical sectioning," Chinese Science Bulletin **59**, 1291–1307 (2014).
[72]M. Saxena, G. Eluru, and S. S. Gorthi, "Structured illumination microscopy," Adv. Opt. Photonics **7**, 241 (2015).
[73]Y. Wu and H. Shroff, "Faster, sharper, and deeper: Structured illumination microscopy for biological imaging," Nat. Methods **15**, 1011–1019 (2018).
[74]E. McLeod and A. Ozcan, "Unconventional methods of imaging: Computational microscopy and compact implementations," Rep. Prog. Phys. **79**, 076001 (2016).
[75]G. Zheng, C. Kolner, and C. Yang, "Microscopy refocusing and dark-field imaging by using a simple LED array," Opt. Lett. **15**, 3987–3989 (2011).
[76]G. Zheng, R. Horstmeyer, and C. Yang, "Wide-field, high-resolution Fourier ptychographic microscopy," Nat. Photonics **7**, 739–745 (2013).
[77]L. Tian, J. Wang, and L. Waller, "3D differential phase-contrast microscopy with computational illumination using an LED array," Opt. Lett. **39**, 1326 (2014).
[78]Z. Liu, L. Tian, S. Liu, and L. Waller, "Real-time brightfield, darkfield, and phase contrast imaging in a light-emitting diode array microscope," J. Biomed. Opt. **19**, 106002 (2014).
[79]K. Ramchandran, L. Waller, L. Tian, and X. Li, "Multiplexed coded illumination for Fourier Ptychography with an LED array microscope," Biomed. Opt. Express **5**, 2376–2389 (2014).
[80]C. Pontiggia, E. Piano, and L. Repetto, "Lensless digital holographic microscope with light-emitting diode illumination," Opt. Lett. **29**, 1132–1134 (2004).
[81]A. Greenbaum, U. Sikora, and A. Ozcan, "Field-portable wide-field microscopy of dense samples using multi-height pixel super-resolution based lensfree imaging," Lab Chip **12**, 1242–1245 (2012).
[82]A. Greenbaum, W. Luo, B. Khademhosseinieh, T. W. Su, A. F. Coskun, and A. Ozcan, "Increased space-bandwidth product in pixel super-resolved lensfree on-chip microscopy," Sci. Rep. **3**, 1717 (2013).

[83]F. Kazemzadeh, C. Jin, S. Molladavoodi, Y. Mei, M. B. Emelko, M. B. Gorbet, and A. Wong, "Lens-free spectral light-field fusion microscopy for contrast- and resolution-enhanced imaging of biological specimens," Opt. Lett. **40**, 3862 (2015).
[84]G. Scholz, S. Mariana, A. B. Dharmawan, I. Syamsu, P. Hörmann, C. Reuse, J. Hartmann, K. Hiller, J. D. Prades, H. S. Wasisto, and A. Waag, "Continuous live-cell culture imaging and single-cell tracking by computational lensfree LED microscopy," Sensors **19**, 1234 (2019).
[85]J. Zhang, J. Sun, Q. Chen, and C. Zuo, "Resolution analysis in a lens-free on-chip digital holographic microscope," IEEE Trans. Comput. Imaging **6**, 697–710 (2020).
[86]S. So, M. Kim, D. Lee, D. M. Nguyen, and J. Rho, "Overcoming diffraction limit: From microscopy to nanoscopy," Appl. Spectrosc. Rev. **53**, 290–312 (2018).
[87]E. Sezgin, "Super-resolution optical microscopy for studying membrane structure and dynamics," J. Phys.: Condens. Matter **29**, 273001 (2017).
[88]J. S. Verdaasdonk, A. D. Stephens, J. Haase, and K. Bloom, "Bending the rules: Widefield microscopy and the abbe limit of resolution," J. Cell. Physiol. **229**, 132–138 (2014).
[89]E. Abbe, "Beiträge zur Theorie des Mikroskops und der mikroskopischen Wahrnehmung," Arch. Mikrosk. Anat. **9**, 413–468 (1873).
[90]D. D. Bezshlyakh, H. Spende, T. Weimann, P. Hinze, S. Bornemann, J. Gülink, J. Canals, J. D. Prades, A. Dieguez, and A. Waag, "Directly addressable GaN-based nano-LED arrays: Fabrication and electro-optical characterization," Microsyst. Nanoeng. **6**, 88 (2020).
[91]M. Mikulics, J. Mayer, and H. H. Hardtdegen, "Cutting-edge nano-LED technology," J. Appl. Phys. **131**, 110903 (2022).
[92]K. Ogawa, R. Hachiya, T. Mizutani, S. Ishijima, and A. Kikuchi, "Fabrication of InGaN/GaN MQW nano-LEDs by hydrogen-environment anisotropic thermal etching," Phys. Status Solidi A **214**, 1600613 (2017).
[93]N. Franch, J. Canals, V. Moro, A. Vilá, A. Romano-Rodríguez, J. D. Prades, J. Gülink, D. Bezshlyakh, A. Waag, K. Kluczyk-Korch, M. Auf der Maur, A. di Carlo, and Á. Diéguez, "Nano illumination microscopy: A technique based on scanning with an array of individually addressable nanoLEDs," Opt. Express **28**, 19044 (2020).
[94]K. Kluczyk-Korch, D. Palazzo, A. Waag, A. Diéguez, J. D. Prades, A. Di Carlo, and M. Auf der Maur, "Optical design of InGaN/GaN nanoLED arrays on a chip: Toward: Highly resolved illumination," Nanotechnology **32**, 105203 (2020).
[95]S. Suzuki and Y. Matsumoto, "Lithography with UV-LED array for curved surface structure," in Microsyst. Technol. **14**, 1291–1297 (2008).
[96]B. Guilhabert, D. Massoubre, E. Richardson, J. J. McKendry, G. Valentine, R. K. Henderson, I. M. Watson, E. Gu, and M. D. Dawson, "Sub-micron lithography using InGaN micro-LEDs: Mask-free fabrication of LED arrays," IEEE Photonics Technol. Lett. **24**, 2221–2224 (2012).
[97]R. M. Guijt and M. C. Breadmore, "Maskless photolithography using UV LEDs," Lab Chip **8**, 1402–1404 (2008).
[98]M.-C. Wu and I.-T. Chen, "High-resolution 960 × 540 and 1920 × 1080 UV micro light-emitting diode displays with the application of maskless photolithography," Adv. Photonics Res. **2**, 2100064 (2021).
[99]J.-E. Ryu, S. Park, Y. Park, S.-W. Ryu, K. Hwang, and H. Won Jang, "Technological breakthroughs in chip fabrication, transfer, and color conversion for high performance micro-LED display," Adv. Mater. (published online, 2022).
[100]F. Olivier, A. Daami, C. Licitra, and F. Templier, "Shockley-Read-Hall and Auger non-radiative recombination in GaN based LEDs: A size effect study," Appl. Phys. Lett. **111**, 022104 (2017).
[101]M. Zhu, S. You, T. Detchprohm, T. Paskova, E. A. Preble, and C. Wetzel, "Various misfit dislocations in green and yellow GaInN/GaN light emitting diodes," Phys. Status Solidi A **207**, 1305–1308 (2010).
[102]T. Detchprohm, Y. Xia, Y. Xi, M. Zhu, W. Zhao, Y. Li, E. F. Schubert, L. Liu, D. Tsvetkov, D. Hanser, and C. Wetzel, "Dislocation analysis in homoepitaxial GaInN/GaN light emitting diode growth," J. Cryst. Growth **298**, 272–275 (2007).
[103]G. Liu, H. Zhao, J. Zhang, J. D. Poplawsky, N. Tansu, and V. Dierolf, "Approaches for high internal quantum efficiency green InGaN light-emitting diodes with large overlap quantum wells," Opt. Express **19**, A991–A1007 (2011).
[104]P. Tian, J. J. D. McKendry, Z. Gong, B. Guilhabert, I. M. Watson, E. Gu, Z. Chen, G. Zhang, and M. D. Dawson, "Size-dependent efficiency and efficiency droop of blue InGaN micro-light emitting diodes," Appl. Phys. Lett. **101**, 231110 (2012).
[105]F. Olivier, S. Tirano, L. Dupré, B. Aventurier, C. Largeron, and F. Templier, "Influence of size-reduction on the performances of GaN-based micro-LEDs for display application," J. Luminescence **191**, 112–116 (2017).
[106]S. Hang, C. M. Chuang, Y. Zhang, C. Chu, K. Tian, Q. Zheng, T. Wu, Z. Liu, Z. H. Zhang, Q. Li, and H. C. Kuo, "A review on the low external quantum efficiency and the remedies for GaN-based micro-LEDs," J. Phys. D **54**, 153002 (2021).
[107]H. Zhao, G. Liu, J. Zhang, R. A. Arif, and N. Tansu, "Analysis of internal quantum efficiency and current injection efficiency in III-nitride light-emitting diodes," J. Disp. Technol. **9**, 212–225 (2013).
[108]S. Nakamura, "The roles of structural imperfections in InGaN-based blue light-emitting diodes and laser diodes," Science **281**, 956–961 (1998).
[109]Y. Liao, C. Thomidis, C. K. Kao, and T. D. Moustakas, "AlGaN based deep ultraviolet light emitting diodes with high internal quantum efficiency grown by molecular beam epitaxy," Appl. Phys. Lett. **98**, 081110 (2011).
[110]E. F. Schubert, *Light-Emitting Diodes* (Cambridge University Press, 2006), p. 422.
[111]P. Degenaar, N. Grossman, M. A. Memon, J. Burrone, M. Dawson, E. Drakakis, M. Neil, and K. Nikolic, "Optobionic vision-a new genetically enhanced light on retinal prosthesis," J. Neural Eng. **6**, 035007 (2009).
[112]T. Ishizuka, M. Kakuda, R. Araki, and H. Yawo, "Kinetic evaluation of photosensitivity in genetically engineered neurons expressing green algae light-gated channels," Neurosci. Res. **54**, 85–94 (2006).
[113]H. Yang, J. W. M. Bergmans, T. C. W. Schenk, J.-P. M. G. Linnartz, and R. Rietman, "An analytical model for the illuminance distribution of a power LED," Opt. Express **16**, 21641–21646 (2008).
[114]L. Svilainis and V. Dumbrava, "LED far field pattern approximation performance study," in *2007 29th International Conference on Information Technology Interfaces* (IEEE, 2007), pp. 645–649.
[115]Y. Chen, B. Xiong, Y. Xue, X. Jin, X. Jin, J. Greene, L. Tian, and L. Tian, "Design of a high-resolution light field miniscope for volumetric imaging in scattering tissue," Biomed. Opt. Express **11**, 1662–1678 (2020).
[116]W.-S. Sun, C.-L. Tien, C.-H. Ma, and J.-W. Pan, "Compact LED projector design with high uniformity and efficiency," Appl. Opt. **53**, H227 (2014).
[117]P. P. Iyer, R. A. DeCrescent, Y. Mohtashami, G. Lheureux, N. A. Butakov, A. Alhassan, C. Weisbuch, S. Nakamura, S. P. DenBaars, and J. A. Schuller, "Unidirectional luminescence from InGaN/GaN quantum-well metasurfaces," Nat. Photonics **14**, 543–548 (2020).
[118]J. Huang, Z. Hu, X. Gao, Y. Xu, and L. Wang, "Unidirectional-emitting GaN-based micro-LED for 3D display," Opt. Lett. **46**, 3476 (2021).
[119]C. L. Liao, C. L. Ho, Y. F. Chang, C. H. Wu, and M. C. Wu, "High-Speed light-emitting diodes emitting at 500 nm with 463-mhz modulation bandwidth," IEEE Electron Device Lett. **35**, 563–565 (2014).
[120]R. X. Ferreira, E. Xie, J. J. D. McKendry, S. Rajbhandari, H. Chun, G. Faulkner, S. Watson, A. E. Kelly, E. Gu, R. V. Penty, I. H. White, D. C. O'Brien, and M. D. Dawson, "High bandwidth GaN-based micro-LEDs for multi-Gb/s visible light communications," IEEE Photonics Technol. Lett. **28**, 2023–2026 (2016).
[121]S.-C. Zhu, L.-X. Zhao, C. Yang, H.-C. Cao, Z.-G. Yu, and L. Liu, "GaN-based flip-chip parallel micro LED array for visible light communication," Proc. SPIE **10244**, 102441Y (2017).
[122]H. Huang, H. Wu, C. Huang, Z. Chen, C. Wang, Z. Yang, and H. Wang, "Characteristics of micro-size light-emitting diode for illumination and visible light communication," Phys. Status Solidi A **215**, 1800484 (2018).
[123]H. Chun, P. Manousiadis, S. Rajbhandari, D. A. Vithanage, G. Faulkner, D. Tsonev, J. J. D. McKendry, S. Videv, E. Xie, E. Gu, M. D. Dawson, H. Haas, G. A. Turnbull, I. D. W. Samuel, and D. C. O'Brien, "Visible light communication using a blue GaN μLED and fluorescent polymer color converter," IEEE Photonics Technol. Lett. **26**, 2035–2038 (2014).
[124]S. Mei, X. Liu, W. Zhang, R. Liu, L. Zheng, R. Guo, and P. Tian, "High-bandwidth white-light system combining a micro-LED with perovskite quantum

dots for visible light communication," ACS Appl. Mater. Interfaces **10**, 5641–5648 (2018).
[125]S. Shim, W. B. Park, M. Kim, J. W. Lee, S. P. Singh, and K. S. Sohn, "Cyan-light-emitting chalcogenometallate phosphor, $KGaS_2$:Eu^{2+}, for phosphor-converted white light-emitting diodes," Inorg. Chem. **60**, 6047–6056 (2021).
[126]J. Bae, Y. Shin, H. Yoo, Y. Choi, J. Lim, D. Jeon, I. Kim, M. Han, and S. Lee, "Quantum dot-integrated GaN light-emitting diodes with resolution beyond the retinal limit," Nat. Commun. **13**, 1862 (2022).
[127]H. Song and S. Lee, "Red light emitting solid state hybrid quantum dot-near-UV GaN LED devices," Nanotechnology **18**, 255202 (2007).
[128]Y.-H. Chang, Y.-M. Huang, F.-J. Liou, C.-W. Chow, Y. Liu, H.-C. Kuo, C.-H. Yeh, W. H. Gunawan, T.-Y. Hung, and Y.-H. Jian, "2.805 Gbit/s high-bandwidth phosphor white light visible light communication utilizing an InGaN/GaN semipolar blue micro-LED," Opt. Express **30**, 16938 (2022).
[129]Z. L. Fang, Q. F. Li, X. Y. Shen, H. Xiong, J. F. Cai, J. Y. Kang, and W. Z. Shen, "Modified InGaN/GaN quantum wells with dual-wavelength green-yellow emission," J. Appl. Phys. **115**, 043514 (2014).
[130]K. Deisseroth and P. Hegemann, "The form and function of channelrhodopsin," Science **357**, aan5544 (2017).
[131]L. Grosenick, J. H. Marshel, and K. Deisseroth, "Closed-loop and activity-guided optogenetic control," Neuron **86**, 106–139 (2015).
[132]F. Schneider, C. Grimm, and P. Hegemann, "Biophysics of channelrhodopsin," Annu. Rev. Biophys. **44**, 167–186 (2015).
[133]F. Zhang, J. Vierock, O. Yizhar, L. E. Fenno, S. Tsunoda, A. Kianianmomeni, M. Prigge, A. Berndt, J. Cushman, J. Polle, J. Magnuson, P. Hegemann, and K. Deisseroth, "The microbial opsin family of optogenetic tools," Cell **147**, 1446–1457 (2011).
[134]N. C. Klapoetke, Y. Murata, S. S. Kim, S. R. Pulver, A. Birdsey-Benson, Y. K. Cho, T. K. Morimoto, A. S. Chuong, E. J. Carpenter, Z. Tian, J. Wang, Y. Xie, Z. Yan, Y. Zhang, B. Y. Chow, B. Surek, M. Melkonian, V. Jayaraman, M. Constantine-Paton, G. K. S. Wong, and E. S. Boyden, "Independent optical excitation of distinct neural populations," Nat. Methods **11**, 338–346 (2014).
[135]J. Marshall, T. W. Cronin, and S. Kleinlogel, "Stomatopod eye structure and function: A review," Arthropod Struct. Dev. **36**, 420–448 (2007).
[136]W. Wang, Z. Nossoni, T. Berbasova, C. T. Watson, I. Yapici, K. S. S. Lee, C. Vasileiou, J. H. Geiger, and B. Borhan, "Tuning the electronic absorption of protein-embedded all-*trans*-retinal," Science **338**, 1340–1343 (2012).
[137]R. O. Lussow, "Photoresist materials and applications," J. Vac. Sci. Technol. **6**, 18 (2000).
[138]C. Luo, C. Xu, L. Lv, H. Li, X. Huang, and W. Liu, "Review of recent advances in inorganic photoresists," RSC Adv. **10**, 8385–8395 (2020).
[139]S. Lu, Y. Zhang, Z. H. Zhang, B. Zhu, H. Zheng, S. T. Tan, and H. V. Demir, "High-performance triangular miniaturized-LEDs for high current and power density applications," ACS Photonics **8**, 2304–2310 (2021).
[140]K. Tadatomo, H. Okagawa, Y. Ohuchi, T. Tsunekawa, T. Jyouichi, Y. Imada, M. Kato, H. Kudo, and T. Taguchi, "High output power InGaN ultraviolet light-emitting diodes fabricated on patterned substrates using metalorganic vapor phase epitaxy," Phys. Status Solidi A **188**, 121–125 (2001).
[141]Z. Gong, S. Jin, Y. Chen, J. McKendry, D. Massoubre, I. M. Watson, E. Gu, and M. D. Dawson, "Size-dependent light output, spectral shift, and self-heating of 400 nm InGaN light-emitting diodes," J. Appl. Phys. **107**, 013103 (2010).
[142]S. J. Oh and J. Cho, "Junction temperature rise due to self-heating effects in GaInN blue light-emitting diodes," Thin Solid Films **641**, 8–11 (2017).
[143]J. M. Smith, R. Ley, M. S. Wong, Y. H. Baek, J. H. Kang, C. H. Kim, M. J. Gordon, S. Nakamura, J. S. Speck, and S. P. Denbaars, "Comparison of size-dependent characteristics of blue and green InGaN microLEDs down to 1 μm in diameter," Appl. Phys. Lett. **116**, 071102 (2020).
[144]P. Gibart, "Metal organic vapour phase epitaxy of GaN and lateral overgrowth," Rep. Prog. Phys. **67**, 667–715 (2004).
[145]T. Mukai, K. Takekawa, and S. Nakamura, "InGaN-based blue light-emitting diodes grown on epitaxially laterally overgrown GaN substrates," Jpn. J. Appl. Phys., Part II **37**, L839 (1998).
[146]Y. P. Hsu, S. J. Chang, Y. K. Su, J. K. Sheu, C. T. Lee, T. C. Wen, L. W. Wu, C. H. Kuo, C. S. Chang, and S. C. Shei, "Lateral epitaxial patterned sapphire InGaN/GaN MQW LEDs," J. Cryst. Growth **261**, 466–470 (2004).
[147]E. F. Schubert and J. K. Kim, "Solid-state light sources getting smart," Science **308**, 1274–1278 (2005).
[148]J. J. Wierer, Jr., A. David, and M. M. Megens, "III-nitride photonic-crystal light-emitting diodes with high extraction efficiency," Nat. Photonics **3**, 163–169 (2009).
[149]D. Ge, X. Huang, J. Wei, P. Qian, L. Zhang, J. Ding, and S. Zhu, "Improvement of light extraction efficiency in GaN-based light-emitting diodes by addition of complex photonic crystal structure," Mater. Res. Express **6**, 086201 (2019).
[150]Y.-C. Lee, C.-H. Ni, and C.-Y. Chen, "Enhancing light extraction mechanisms of GaN-based light-emitting diodes through the integration of imprinting microstructures, patterned sapphire substrates, and surface roughness," Opt. Express **18**, A489 (2010).
[151]G. D. Hao and X. L. Wang, "Enhancement of light extraction efficiency by evanescent wave coupling effect in ridge-shaped AlGaInP/GaInP quantum wells," Appl. Phys. Lett. **100**, 091107 (2012).
[152]P. P. Maaskant, E. A. O'carroll, P. M. Lambkin, and B. Corbett, "Light emitting mesa structures with high aspect ratio and near-parabolic sidewalls," U.S. patent 7,518,149 (2009).
[153]E. Matioli, E. Rangel, M. Iza, B. Fleury, N. Pfaff, J. Speck, E. Hu, and C. Weisbuch, "High extraction efficiency light-emitting diodes based on embedded air-gap photonic-crystals," Appl. Phys. Lett. **96**, 031108 (2010).
[154]J. J. Wierer, M. R. Krames, J. E. Epler, N. F. Gardner, M. G. Craford, J. R. Wendt, J. A. Simmons, and M. M. Sigalas, "InGaN/GaN quantum-well heterostructure light-emitting diodes employing photonic crystal structures," Appl. Phys. Lett. **84**, 3885–3887 (2004).
[155]E. Yablonovitch, "Inhibited spontaneous emission in solid-state physics and electronics," Phys. Rev. Lett. **58**, 2059 (1987).
[156]T. N. Oder, K. H. Kim, J. Y. Lin, and H. X. Jiang, "III-nitride blue and ultraviolet photonic crystal light emitting diodes," Appl. Phys. Lett. **84**, 466–468 (2004).
[157]D. H. Kim, C. O. Cho, Y. G. Roh, H. Jeon, Y. S. Park, J. Cho, J. S. Im, C. Sone, Y. Park, W. J. Choi, and Q. H. Park, "Enhanced light extraction from GaN-based light-emitting diodes with holographically generated two-dimensional photonic crystal patterns," Appl. Phys. Lett. **87**, 203508 (2005).
[158]K. J. Byeon, S. Y. Hwang, and H. Lee, "Fabrication of two-dimensional photonic crystal patterns on GaN-based light-emitting diodes using thermally curable monomer-based nanoimprint lithography," Appl. Phys. Lett. **91**, 091106 (2007).
[159]K. McGroddy, A. David, E. Matioli, M. Iza, S. Nakamura, S. Denbaars, J. S. Speck, C. Weisbuch, and E. L. Hu, "Directional emission control and increased light extraction in GaN photonic crystal light emitting diodes," Appl. Phys. Lett. **93**, 103502 (2008).
[160]A. David, C. Meier, R. Sharma, F. S. Diana, S. P. Denbaars, E. Hu, S. Nakamura, C. Weisbuch, and H. Benisty, "Photonic bands in two-dimensionally patterned multimode GaN waveguides for light extraction," Appl. Phys. Lett. **87**, 101107 (2005).
[161]A. David, T. Fujii, R. Sharma, K. McGroddy, S. Nakamura, S. P. Denbaars, E. L. Hu, C. Weisbuch, and H. Benisty, "Photonic-crystal GaN light-emitting diodes with tailored guided modes distribution," Appl. Phys. Lett. **88**, 061124 (2006).
[162]I. Schnitzer, E. Yablonovitch, C. Caneau, T. J. Gmitter, and A. Scherer, "30 efficiency from diodes," Appl. Phys. Lett. **63**, 2174–2176 (1993).
[163]R. Windisch, C. Rooman, S. Meinlschmidt, P. Kiesel, D. Zipperer, G. H. Döhler, B. Dutta, M. Kuijk, G. Borghs, and P. Heremans, "Impact of texture-enhanced transmission on high-efficiency surface-textured light-emitting diodes," Appl. Phys. Lett. **79**, 2315–2317 (2001).
[164]C. Huh, K. S. Lee, E. J. Kang, and S. J. Park, "Improved light-output and electrical performance of InGaN-based light-emitting diode by microroughening of the *p*-GaN surface," J. Appl. Phys. **93**, 9383–9385 (2003).
[165]T. Fujii, Y. Gao, R. Sharma, E. L. Hu, S. P. DenBaars, and S. Nakamura, "Increase in the extraction efficiency of GaN-based light-emitting diodes via surface roughening," Appl. Phys. Lett. **84**, 855–857 (2004).
[166]W. C. Peng and Y. C. S. Wu, "Improved luminance intensity of InGaN-GaN light-emitting diode by roughening both the *p*-GaN surface and the undoped-GaN surface," Appl. Phys. Lett. **89**, 041116 (2006).
[167]C. M. Tsai, J. K. Sheu, W. C. Lai, Y. P. Hsu, P. T. Wang, C. T. Kuo, C. W. Kuo, S. J. Chang, and Y. K. Su, "Enhanced output power in GaN-based LEDs with

naturally textured surface grown by MOCVD," IEEE Electron Device Lett. **26**, 464–466 (2005).
[168]H. W. Huang, C. C. Kao, J. T. Chu, W. D. Liang, H. C. Kuo, S. C. Wang, and C. C. Yu, "Improvement of InGaN/GaN light emitting diode performance with a nano-roughened p-GaN surface by excimer laser-irradiation," Mater. Chem. Phys. **99**, 414–417 (2006).
[169]T.-L. Chang, Z.-C. Chen, and Y.-C. Lee, "Micro/nano structures induced by femtosecond laser to enhance light extraction of GaN-based LEDs," Opt. Express **20**, 15997 (2012).
[170]H. Wang, L. Wang, J. Sun, T. L. Guo, E. G. Chen, X. T. Zhou, Y. A. Zhang, and Q. Yan, "Role of surface microstructure and shape on light extraction efficiency enhancement of GaN micro-LEDs: A numerical simulation study," Displays **73**, 102172 (2022).
[171]R. Windisch, B. Dutta, M. Kuijk, A. Knobloch, S. Meinlschmidt, S. Schoberth, P. Kiesel, G. Borghs, G. H. Döhler, and P. Heremans, "40 optimization of natural lithography," IEEE Trans. Electron Devices **47**, 1492–1498 (2000).
[172]R. H. Horng, C. C. Yang, J. Y. Wu, S. H. Huang, C. E. Lee, and D. S. Wuu, "GaN-based light-emitting diodes with indium tin oxide texturing window layers using natural lithography," Appl. Phys. Lett. **86**, 221101 (2005).
[173]M. Yamada, T. Mitani, Y. Narukawa, S. Shioji, I. Niki, S. Sonobe, K. Deguchi, M. Sano, and T. Mukai, "InGaN-based near-ultraviolet and blue-light-emitting diodes with high external quantum efficiency using a patterned sapphire substrate and a mesh electrode," Jpn. J. Appl. Phys. **41**, L1431–L1433 (2002).
[174]S. J. Chang, Y. C. Lin, Y. K. Su, C. S. Chang, T. C. Wen, S. C. Shei, J. C. Ke, C. W. Kuo, S. C. Chen, and C. H. Liu, "Nitride-based LEDs fabricated on patterned sapphire substrates," Solid-State Electron. **47**, 1539–1542 (2003).
[175]Y. J. Lee, H. C. Kuo, T. C. Lu, B. J. Su, and S. C. Wang, "Fabrication and characterization of GaN-based LEDs grown on chemical wet-etched patterned sapphire substrates," J. Electrochem. Soc. **153**, G1106 (2006).
[176]C.-T. Chang, S.-K. Hsiao, E. Y. Chang, Y.-L. Hsiao, J.-C. Huang, C.-Y. Lu, H.-C. Chang, K.-W. Cheng, and C.-T. Lee, "460-nm InGaN-based LEDS grown on fully inclined hemisphere-shape-patterned sapphire substrate with submicrometer spacing," IEEE Photonics Technol. Lett. **21**, 1366–1368 (2009).
[177]J. Wang, L. W. Guo, H. Q. Jia, Z. G. Xing, Y. Wang, J. F. Yan, N. S. Yu, H. Chen, and J. M. Zhou, "Investigation of characteristics of laterally overgrown GaN on striped sapphire substrates patterned by wet chemical etching," J. Cryst. Growth **290**, 398–404 (2006).
[178]W.-C. Ke, C.-Y. Chiang, W. Son, and F.-W. Lee, "InGaN-based light-emitting diodes grown on various aspect ratios of concave nanopattern sapphire substrate," Appl. Surf. Sci. **456**, 967–972 (2018).
[179]S. X. Jiang, Z. Z. Chen, X. Z. Jiang, X. X. Fu, S. Jiang, Q. Q. Jiao, T. J. Yu, and G. Y. Zhang, "Study on the morphology and shape control of volcano-shaped patterned sapphire substrates fabricated by imprinting and wet etching," CrystEngComm **17**, 3070–3075 (2015).
[180]J.-J. Chen, Y.-K. Su, C.-L. Lin, S.-M. Chen, W.-L. Li, and C.-C. Kao, "Enhanced output power of GaN-based LEDS with nano-patterned sapphire substrates," IEEE Photonics Technol. Lett. **20**, 1193–1195 (2008).
[181]S. Zhou, X. Zhao, P. Du, Z. Zhang, X. Liu, S. Liu, and L. J. Guo, "Application of patterned sapphire substrate for III-nitride light-emitting diodes," Nanoscale **14**, 4887–4907 (2022).
[182]R. H. Horng, W. K. Wang, S. C. Huang, S. Y. Huang, S. H. Lin, C. F. Lin, and D. S. Wuu, "Growth and characterization of 380-nm InGaN/AlGaN LEDs grown on patterned sapphire substrates," J. Cryst. Growth **298**, 219–222 (2007).
[183]P. Dong, J. Yan, J. Wang, Y. Zhang, C. Geng, T. Wei, P. Cong, Y. Zhang, J. Zeng, Y. Tian, L. Sun, Q. Yan, J. Li, S. Fan, and Z. Qin, "282-nm AlGaN-based deep ultraviolet light-emitting diodes with improved performance on nano-patterned sapphire substrates," Appl. Phys. Lett. **102**, 241113 (2013).
[184]V.-C. Su, P.-H. Chen, R.-M. Lin, M.-L. Lee, Y.-H. You, C.-I. Ho, Y.-C. Chen, W.-F. Chen, and C.-H. Kuan, "Suppressed quantum-confined Stark effect in InGaN-based LEDs with nano-sized patterned sapphire substrates," Opt. Express **21**, 30065 (2013).
[185]H. Gao, F. Yan, Y. Zhang, J. Li, Y. Zeng, and G. Wang, "Enhancement of the light output power of InGaN/GaN light-emitting diodes grown on pyramidal patterned sapphire substrates in the micro- and nanoscale," J. Appl. Phys. **103**, 014314 (2008).
[186]L. Zhu, P. T. Lai, and H. W. Choi, "LED with integrated microlens array patterned by an ultraviolet linear micro-LED array," in *2010 Photonics Global Conference* (IEEE, 2010), pp. 52–54.
[187]B. Demory, K. Chung, A. Katcher, J. Sui, H. Deng, and P. C. Ku, "Integrated parabolic nanolenses on MicroLED color pixels," Nanotechnology **29**, 165201 (2018).
[188]X. Deng, X. Liang, Z. Chen, W. Yu, and R. Ma, "Uniform illumination of large targets using a lens array," Appl. Opt. **25**, 377 (1986).
[189]A. Buüttner, "Wave optical analysis of light-emitting diode beam shaping using microlens arrays," Opt. Eng. **41**, 2393 (2002).
[190]H. W. Choi, E. Gu, J. M. Girkin, and M. D. Dawson, "Nitride micro-display with integrated micro-lenses," Phys. Status Solidi C **2**, 2903–2906 (2005).
[191]X. H. Li, R. Song, Y. K. Ee, P. Kumnorkaew, J. F. Gilchrist, and N. Tansu, "Light extraction efficiency and radiation patterns of III-nitride light-emitting diodes with colloidal microlens arrays with various aspect ratios," IEEE Photonics J. **3**, 489–499 (2011).
[192]G. Wang, L. Wang, F. Li, and D. Kong, "Design of optical element combining Fresnel lens with microlens array for uniform light-emitting diode lighting," J. Opt. Soc. Am. A **29**, 1877 (2012).
[193]X.-H. Lee, I. Moreno, and C.-C. Sun, "High-performance LED street lighting using microlens arrays," Opt. Express **21**, 10612 (2013).
[194]H. S. Park, R. Hoskinson, H. Abdollahi, and B. Stoeber, "Compact near-eye display system using a superlens-based microlens array magnifier," Opt. Express **23**, 30618 (2015).
[195]A. Davis and F. Kühnlenz, "Optical design using Fresnel lenses," Opt. Photonik **2**, 52–55 (2007).
[196]W. A. Parkyn and D. G. Pelka, "Compact nonimaging lens with totally internally reflecting facets," Nonimaging Opt.**1528**, 70–81 (1991).
[197]W. A. Parkyn and D. G. Pelka, "New TIR lens applications for light-emitting diodes," Nonimaging Opt. **3139**, 135–140 (1997).
[198]W.-G. Chen and C.-M. Uang, "Better reading light system with light-emitting diodes using optimized Fresnel lens," Opt. Eng. **45**, 063001 (2006).
[199]C. Moser, T. Mayr, and I. Klimant, "Filter cubes with built-in ultrabright light-emitting diodes as exchangeable excitation light sources in fluorescence microscopy," J. Microsc. **222**, 135–140 (2006).
[200]J. Y. Joo and S. K. Lee, "Miniaturized TIR Fresnel lens for miniature optical LED applications," Int. J. Precis. Eng. Manuf. **10**, 137–140 (2009).
[201]C.-C. Hsieh, P.-Y. Tsai, Y.-H. Li, and C.-W. Fan, "Investigation of the influence of structural parameters of a Fresnel-type lens on the narrowing of light-emitting diode light beams," J. Micro/Nanolithography, MEMS, MOEMS **10**, 033005 (2011).
[202]F. Chen, K. Wang, Z. Qin, D. Wu, X. Luo, and S. Liu, "Design method of high-efficient LED headlamp lens," Opt. Express **18**, 20926 (2010).
[203]J. Jiang, S. To, W. B. Lee, and B. Cheung, "Optical design of a freeform TIR lens for LED streetlight," Optik **121**, 1761–1765 (2010).
[204]L. T. Chen, G. Keiser, Y. R. Huang, and S. L. Lee, "A simple design approach of a Fresnel lens for creating uniform light-emitting diode light distribution patterns," Fiber Integr. Opt. **33**, 360–382 (2014).
[205]N. H. Vu, T. T. Pham, and S. Shin, "LED uniform illumination using double linear Fresnel lenses for energy saving," Energies **10**, 2091 (2017).
[206]L. Nian, X. Pei, Z. Zhao, and X. Wang, "Review of optical designs for light-emitting diode packaging," IEEE Trans. Compon., Packag., Manuf. Technol. **9**, 642–648 (2019).
[207]T. Erdem and H. V. Demir, "Color science of nanocrystal quantum dots for lighting and displays," Nanophotonics **2**, 57–81 (2013).
[208]W. J. Chung and Y. H. Nam, "Review—A review on phosphor in glass as a high power LED color converter," ECS J. Solid State Sci. Technol. **9**, 016010 (2020).
[209]L. Wang, X. Wang, F. Bertram, B. Sheng, Z. Hao, Y. Luo, C. Sun, B. Xiong, Y. Han, J. Wang, H. Li, G. Schmidt, P. Veit, J. Christen, and X. Wang, "Color-tunable 3D InGaN/GaN multi-quantum-well light-emitting-diode based on microfacet emission and programmable driving power supply," Adv. Opt. Mater. **9**, 2001400 (2021).
[210]B. Damilano, N. Grandjean, C. Pernot, and J. Massies, "Monolithic white light emitting diodes based on InGaN/GaN multiple-quantum wells," Jpn. J. Appl. Phys., Part II **40**, L918 (2001).

[211] H. Q. T. Bui, R. T. Velpula, B. Jain, O. H. Aref, H. D. Nguyen, T. R. Lenka, and H. P. T. Nguyen, "Full-color InGaN/AlGaN nanowire micro light-emitting diodes grown by molecular beam epitaxy: A promising candidate for next generation micro displays," Micromachines **10**, 492 (2019).
[212] R. Wang, H. P. T. Nguyen, A. T. Connie, J. Lee, I. Shih, and Z. Mi, "Color-tunable, phosphor-free InGaN nanowire light-emitting diode arrays monolithically integrated on silicon," Opt. Express **22**, A1768–A1775 (2014).
[213] K. Chung, J. Sui, B. Demory, and P. C. Ku, "Color mixing from monolithically integrated InGaN-based light-emitting diodes by local strain engineering," Appl. Phys. Lett. **111**, 041101 (2017).
[214] Y. Shirasaki, G. J. Supran, M. G. Bawendi, and V. Bulović, "Emergence of colloidal quantum-dot light-emitting technologies," Nat. Photonics **7**, 13–23 (2013).
[215] V. Wood and V. Bulović, "Colloidal quantum dot light-emitting devices," Nano Rev. **1**, 5202 (2010).
[216] C. R. Kagan, E. Lifshitz, E. H. Sargent, and D. V. Talapin, "Building devices from colloidal quantum dots," Science **353**, aac5523 (2016).
[217] M. Liu, N. Yazdani, M. Yarema, M. Jansen, V. Wood, and E. H. Sargent, "Colloidal quantum dot electronics," Nat. Electron. **4**, 548–558 (2021).
[218] S. Zhu, Y. Song, J. Wang, H. Wan, Y. Zhang, Y. Ning, and B. Yang, "Photoluminescence mechanism in graphene quantum dots: Quantum confinement effect and surface/edge state," Nano Today **13**, 10–14 (2017).
[219] Z. Liu, C. H. Lin, B. R. Hyun, C. W. Sher, Z. Lv, B. Luo, F. Jiang, T. Wu, C. H. Ho, H. C. Kuo, and J. H. He, "Micro-light-emitting diodes with quantum dots in display technology," Light **9**, 83 (2020).
[220] G. J. Supran, K. W. Song, G. W. Hwang, R. E. Correa, J. Scherer, E. A. Dauler, Y. Shirasaki, M. G. Bawendi, and V. Bulović, "High-performance shortwave-infrared light-emitting devices using core-shell (PbS-CdS) colloidal quantum dots," Adv. Mater. **27**, 1437–1442 (2015).
[221] P. O. Anikeeva, J. E. Halpert, M. G. Bawendi, and V. Bulović, "Quantum dot light-emitting devices with electroluminescence tunable over the entire visible spectrum," Nano Lett. **9**, 2532–2536 (2009).
[222] D. Mao, Z. Xiong, M. Donnelly, and G. Xu, "Brushing-assisted two-color quantum-dot micro-LED array towards bi-directional optogenetics," IEEE Electron Device Lett. **42**, 1504–1507 (2021).
[223] Y.-C. Lin, M. Karlsson, M. Bettinelli, N. Armaroli, and H. Bolink, "Inorganic phosphor materials for lighting," in *Topics in Current Chemistry Collections* (Springer, Cham, 2017), Vol. 374, pp. 309–355.
[224] G. B. Nair, H. C. Swart, and S. J. Dhoble, "A review on the advancements in phosphor-converted light emitting diodes (pc-LEDs): Phosphor synthesis, device fabrication and characterization," Prog. Mater. Sci. **109**, 100622 (2020).
[225] M. Shang, C. Li, and J. Lin, "How to produce white light in a single-phase host?," Chem. Soc. Rev. **43**, 1372–1386 (2014).
[226] Y. Q. Li, N. Hirosaki, R. J. Xie, T. Takeda, and M. Mitomo, "Yellow-orange-emitting $CaAlSiN_3$:Ce^{3+} phosphor: Structure, photoluminescence, and application in white LEDs," Chem. Mater. **20**, 6704–6714 (2008).
[227] K. Asami, M. Shiraiwa, J. Ueda, K. Fujii, K. Hongo, R. Maezono, M. G. Brik, M. Yashima, and S. Tanabe, "Crystal structure analysis and evidence of mixed anion coordination at the Ce^{3+} site in $Y_3Al_2(Al,Si)_3(O,N)_{12}$ oxynitride garnet phosphor," J. Mater. Chem. C **7**, 1330–1336 (2019).
[228] P. Dang, D. Liu, G. Li, A. A. Al Kheraif, and J. Lin, "Recent advances in bismuth ion-doped phosphor materials: Structure design, tunable photoluminescence properties, and application in white LEDs," Adv. Opt. Mater. **8**, 1901993 (2020).
[229] D. Wilhelm, D. Baumann, M. Seibald, K. Wurst, G. Heymann, and H. Huppertz, "Narrow-band red emission in the nitridolithoaluminate $Sr_4[LiAl_{11}N_{14}]$:Eu^{2+}," Chem. Mater. **29**, 1204–1209 (2017).
[230] R. J. Xie, N. Hirosaki, T. Suehiro, F. F. Xu, and M. Mitomo, "A simple, efficient synthetic route to $Sr_2Si_5N_8$:Eu^{2+}-based red phosphors for white light-emitting diodes," Chem. Mater. **18**, 5578–5583 (2006).
[231] H. Chen, L. Ju, L. Zhang, X. Wang, L. Zhang, X. Xu, L. Gao, K. Qiu, and L. Yin, "Exploring a particle-size-reduction strategy of YAG:Ce phosphor via a chemical breakdown method," J. Rare Earths **39**, 938–945 (2021).
[232] D. C. Chen, Z. G. Liu, Z. H. Deng, C. Wang, Y. G. Cao, and Q. L. Liu, "Optimization of light efficacy and angular color uniformity by hybrid phosphor particle size for white light-emitting diode," Rare Met. **33**, 348–352 (2014).
[233] J. Murphy, S. Camardello, M. Doherty, J. Liu, P. Smigelski, and A. Setlur, "11.1: Invited paper: Narrow-band phosphors for next generation miniLED and microLED displays," in *SID Symposium Digest of Technical Papers* (Wiley Online Library, 2021) Vol. 52, pp. 165–168.
[234] N. Zheludev, "The life and times of the LED—A 100-year history," Nat. Photonics **1**, 189–192 (2007).
[235] H. K. Henisch, "Electroluminescence," Rep. Prog. Phys. **27**, 369 (1964).
[236] P. J. Dean, "Electroluminescence in semiconductors," J. Luminescence **12–13**, 83–95 (1976).
[237] F. Decker, F. Prince, and P. Motisuke, "Electroluminescence of III-V single-crystal semiconducting electrodes," J. Appl. Phys. **57**, 2900 (1998).
[238] T. Mukai, M. Yamada, and S. Nakamura, "Current and temperature dependences of electroluminescence of InGaN-based UV/blue/green light-emitting diodes," Jpn. J. Appl. Phys., Part 2 **37**, L1358 (1998).
[239] F. L. Freitas, M. Marques, and L. K. Teles, "First-principles determination of band-to-band electronic transition energies in cubic and hexagonal AlGaInN alloys," AIP Adv. **6**, 085308 (2016).
[240] D. Brunner, H. Angerer, E. Bustarret, F. Freudenberg, R. Höpler, R. Dimitrov, O. Ambacher, and M. Stutzmann, "Optical constants of epitaxial AlGaN films and their temperature dependence," J. Appl. Phys. **82**, 5090–5096 (1997).
[241] T. Araki, Y. Saito, T. Yamaguchi, M. Kurouchi, Y. Nanishi, and H. Naoi, "Radio frequency-molecular beam epitaxial growth of InN epitaxial films on (0001) sapphire and their properties," J. Vac. Sci. Technol. B **22**, 2139 (2004).
[242] M. S. Wong, D. Hwang, A. I. Alhassan, C. Lee, R. Ley, S. Nakamura, and S. P. DenBaars, "High efficiency of III-nitride micro-light-emitting diodes by sidewall passivation using atomic layer deposition," Opt. Express **26**, 21324 (2018).
[243] K. A. Bulashevich and S. Y. Karpov, "Impact of surface recombination on efficiency of III-nitride light-emitting diodes," Phys. Status Solidi RRL **10**, 480–484 (2016).
[244] J.-T. Oh, S.-Y. Lee, Y.-T. Moon, J. H. Moon, S. Park, K. Y. Hong, K. Y. Song, C. Oh, J.-I. Shim, H.-H. Jeong, J.-O. Song, H. Amano, and T.-Y. Seong, "Light output performance of red AlGaInP-based light emitting diodes with different chip geometries and structures," Opt. Express **26**, 11194 (2018).
[245] C. H. Oh, J. I. Shim, and D. S. Shin, "Current- and temperature-dependent efficiency droops in InGaN-based blue and AlGaInP-based red light-emitting diodes," Jpn. J. Appl. Phys., Part 1 **58**, SCCC08 (2019).
[246] D.-H. Lee, S.-Y. Lee, J.-I. Shim, T.-Y. Seong, and H. Amano, "Effects of current, temperature, and chip size on the performance of AlGaInP-based red micro-light-emitting diodes with different contact schemes," ECS J. Solid State Sci. Technol. **10**, 095001 (2021).
[247] A. Dussaigne, F. Barbier, B. Damilano, S. Chenot, A. Grenier, A. M. Papon, B. Samuel, B. Ben Bakir, D. Vaufrey, J. C. Pillet, A. Gasse, O. Ledoux, M. Rozhavskaya, and D. Sotta, "Full InGaN red light emitting diodes," J. Appl. Phys. **128**, 135704 (2020).
[248] P. Li, H. Li, M. S. Wong, P. Chan, Y. Yang, H. Zhang, M. Iza, J. S. Speck, S. Nakamura, and S. P. Denbaars, "Progress of InGaN-based red micro-light emitting diodes," Crystals **12**, 541 (2022).
[249] J. I. Hwang, R. Hashimoto, S. Saito, and S. Nunoue, "Development of InGaN-based red LED grown on (0001) polar surface," Appl. Phys. Express **7**, 071003 (2014).
[250] D. Iida and K. Ohkawa, "Recent progress in red light-emitting diodes by III-nitride materials," Semicond. Sci. Technol. **37**, 013001 (2022).
[251] Y. Ohta, M. C. Guinto, T. Tokuda, M. Kawahara, M. Haruta, H. Takehara, H. Tashiro, K. Sasagawa, H. Onoe, R. Yamaguchi, Y. Koshimizu, K. Isa, T. Isa, K. Kobayashi, Y. M. Akay, M. Akay, and J. Ohta, "Micro-LED array-based photo-stimulation devices for optogenetics in rat and macaque monkey brains," IEEE Access **9**, 127937–127949 (2021).
[252] L. Li, L. Lu, Y. Ren, G. Tang, Y. Zhao, X. Cai, Z. Shi, H. Ding, C. Liu, D. Cheng, Y. Xie, H. Wang, X. Fu, L. Yin, M. Luo, and X. Sheng, "Colocalized, bidirectional optogenetic modulations in freely behaving mice with a wireless dual-color optoelectronic probe," Nat. Commun. **13**, 839 (2022).
[253] J. F. C. Carreira, E. Xie, R. Bian, C. Chen, J. J. D. McKendry, B. Guilhabert, H. Haas, E. Gu, and M. D. Dawson, "On-chip GaN-based dual-color micro-LED arrays and their application in visible light communication," Opt. Express **27**, A1517 (2019).

[254]J. Y. Lin, P. M. Knutsen, A. Muller, D. Kleinfeld, and R. Y. Tsien, "ReaChR: A red-shifted variant of channelrhodopsin enables deep transcranial optogenetic excitation," Nat. Neurosci. **16**, 1499–1508 (2013).
[255]H. Ishio, J. Minowa, and K. Nosu, "Review and status of wavelength-division-multiplexing technology and its application (invited overview)," J. Lightwave Technol. **2**, 448–463 (1984).
[256]M. Zhanghu, Y. Wang, and Z. Liu, "Compound semiconductor micro-LED array and its novel applications in phototherapy," in *SID Symposium Digest of Technical Papers* (Wiley, 2020), Vol. 51, pp. 121–124.
[257]H. E. Lee, "Next-generation biomedical devices via microLEDS," J. Korean Inst. Electr. Electron. Mater. Eng. **34**, 221–228 (2021).
[258]R. T. Ley, J. M. Smith, M. S. Wong, T. Margalith, S. Nakamura, S. P. DenBaars, and M. J. Gordon, "Revealing the importance of light extraction efficiency in INGaN/GaN microLEDS via chemical treatment and dielectric passivation," Appl. Phys. Lett. **116**, 251104 (2020).
[259]T.-Y. Seong and H. Amano, "Surface passivation of light emitting diodes: From nano-size to conventional mesa-etched devices," Surf. Interfaces **21**, 100765 (2020).
[260]J. Park, W. Baek, D.-M. Geum, and S. Kim, "Understanding the sidewall passivation effects in AlGaInP/GaInP micro-LED," Nanoscale Res. Lett. **17**, 29 (2022).
[261]P. Kirilenko, D. Iida, Z. Zhuang, and K. Ohkawa, "InGaN-based green micro-LED efficiency enhancement by hydrogen passivation of the p-GaN sidewall," Appl. Phys. Express **15**, 084003 (2022).
[262]H. Robbins, K. Sumitomo, N. Tsujimura, and T. Kamei, "Integrated thin film Si fluorescence sensor coupled with a GaN microled for microfluidic point-of-care testing," J. Micromech. Microeng. **28**, 024001 (2017).
[263]J. Park, J. Kim, S.-Y. Kim, W. H. Cheong, J. Jang, Y.-G. Park, K. Na, Y.-T. Kim, J. H. Heo, C. Y. Lee *et al.*, "Soft, smart contact lenses with integrations of wireless circuits, glucose sensors, and displays," Sci. Adv. **4**, eaap9841 (2018).
[264]K. Lee, I. Cho, M. Kang, J. Jeong, M. Choi, K. Y. Woo, K.-J. Yoon, Y.-H. Cho, and I. Park, "Ultra-low-power e-nose system based on multi-micro-led-integrated, nanostructured gas sensors and deep learning," ACS Nano **17**, 539–551 (2022).